

An Ocean Surface Wind Vector Model Function for a Spaceborne Microwave Radiometer and Its Application

Seubson Soisuvann

Final Examination for the degree of
Doctor of Philosophy in Electrical Engineering
November 3, 2006

Presentation Outline

- Dissertation Objective
- Background
 - Brief history of wind observation from space
 - Planck's Blackbody radiation
 - Passive microwave measurement
 - Active microwave measurement
- ADEOS-II satellite
 - AMSR → brightness temperature
 - SeaWinds scatterometer → wind vector
- Dataset collocation

Presentation Outline -2

- Atmospheric independence
- Passive wind vector model function
 - AV-H
 - Model variance
- Model function application
 - Combined passive and fore-look scatterometer for wind direction retrieval
- Conclusion
- List of Publications

Dissertation Objective

- To characterize the passive wind direction signature for vertical and horizontal polarizations
 - Develop passive wind vector model function
- Secondary objective
 - To evaluate combined passive and active wind direction retrieval
 - Fore-look scatterometer

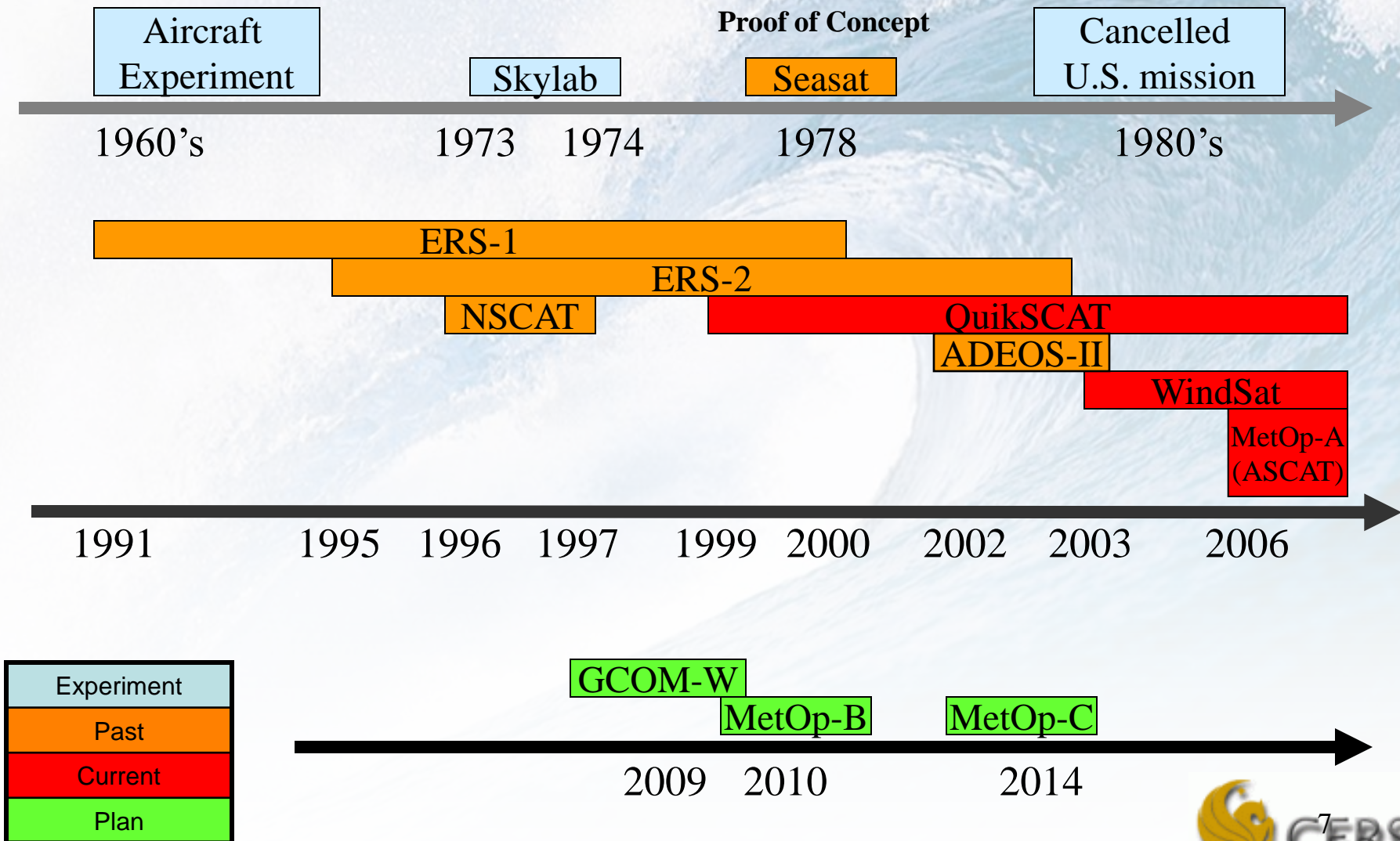
A dramatic photograph of a large, curling blue wave crashing over a rocky shore. The water is a deep, vibrant blue, and the foam is bright white. The wave is curling over, creating a tunnel-like effect. The sky is a clear, bright blue with some light clouds. The overall scene is dynamic and powerful.

Background

Why measure ocean vector wind?

- Ocean circulation science
- Weather forecasting
- Long-term global climate change science
- Ship routing
- Coastal flooding
- Oil production
- Fishing production

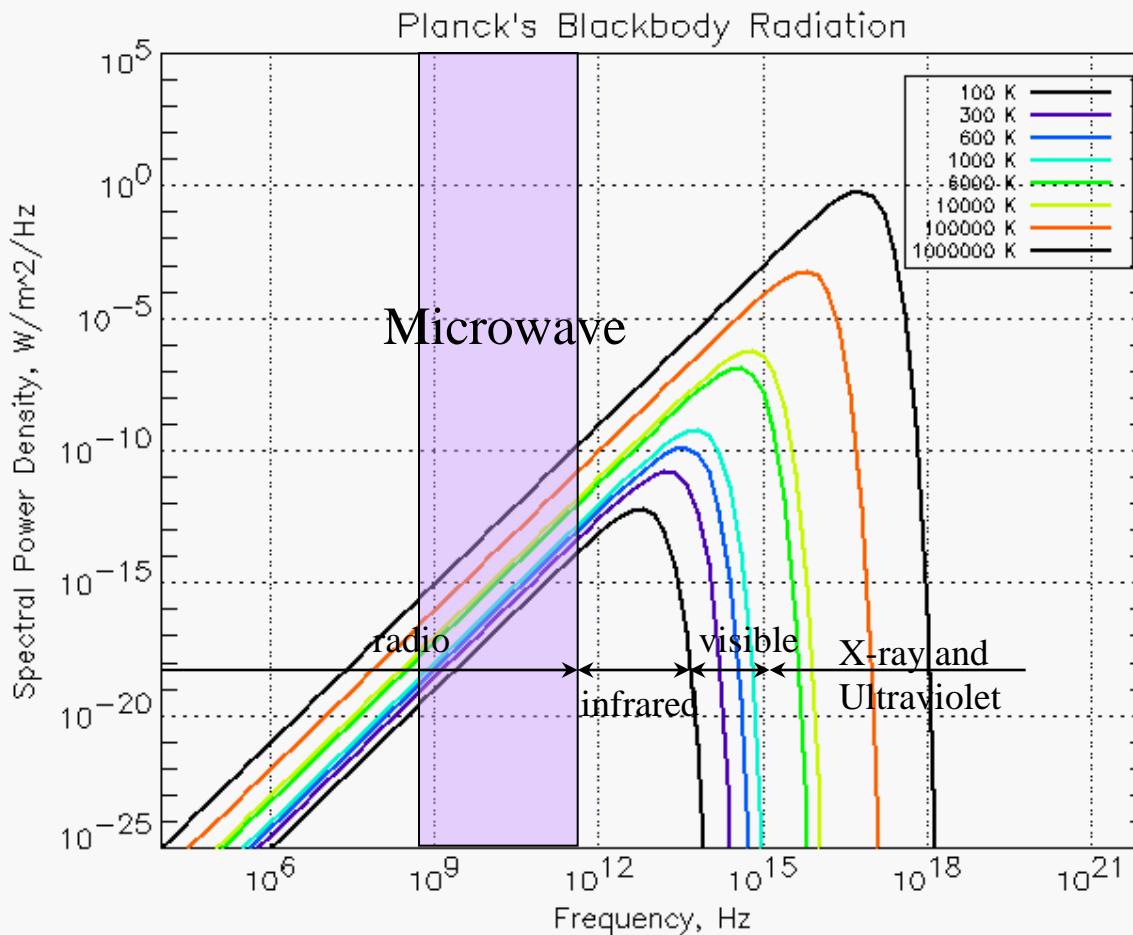
Wind observation satellite missions



Wind measurement technology

- Active Microwave
 - SASS (Seasat)
 - AMI (ERS-1,2)
 - NSCAT (ADEOS-I)
 - SeaWinds (QuikSCAT, ADEOS-II)
 - ASCAT (MetOp-A)
 - Normalized radar cross-section (NRSC) or sigma-0 (σ^0) measurement
- Passive Microwave
 - WindSat (Coriolis)
 - Polarimetric system
 - 3rd and 4th Stokes parameter
 - **New System**
 - Require only linear polarization (V and H)

Planck's Blackbody Radiation



$$S_f = \frac{2\pi h f^3}{c^2} \left(\frac{1}{e^{hf/kT} - 1} \right)$$

k = Boltzmann's constant
 $= 1.38 \times 10^{-23} \text{ J/K}$

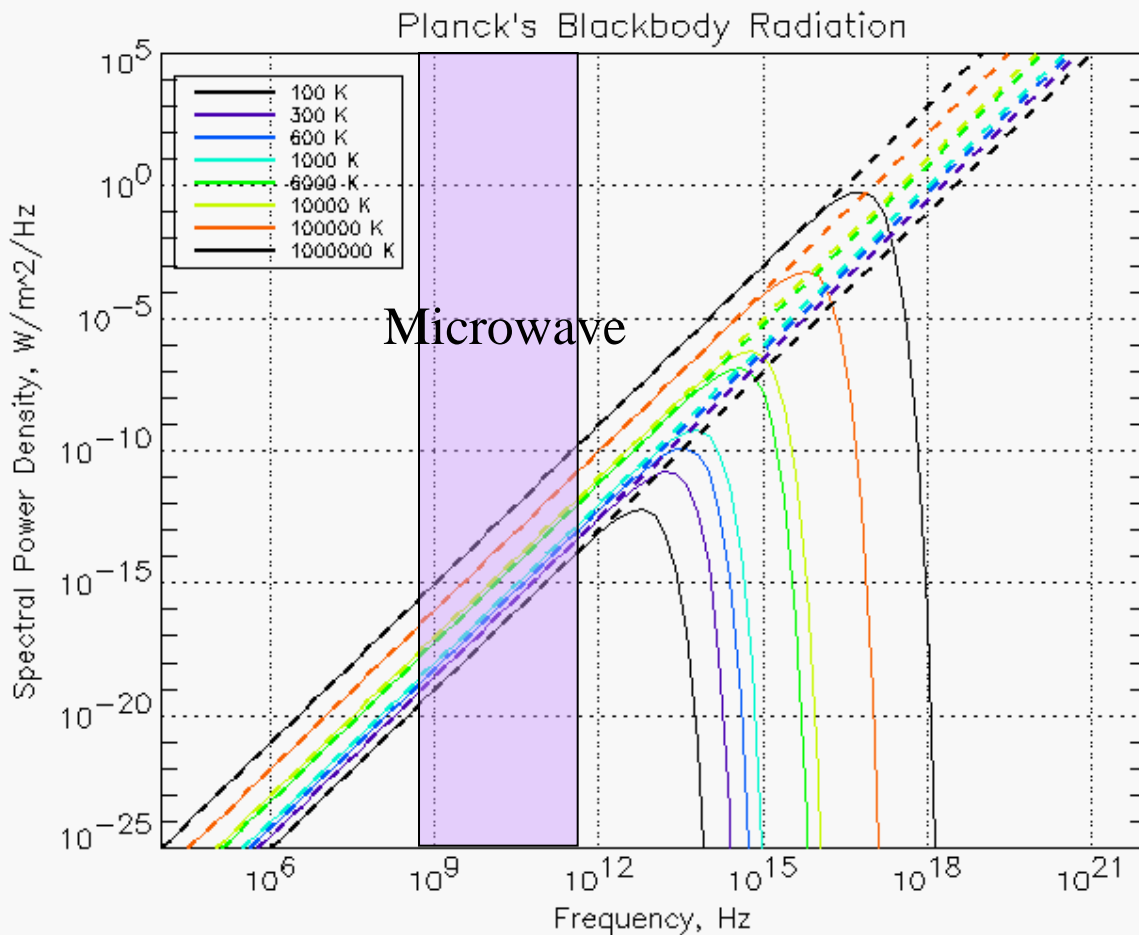
h = Planck's constant
 $= 6.63 \times 10^{-34} \text{ J}$

c = light speed $= 3 \times 10^8 \text{ m/s}$

f = EM frequency, Hz

T = absolute temperature, K

Rayleigh-Jeans Law



$$S_f = \frac{2\pi h f^3}{c^2} \left(\frac{1}{e^{hf/kT} - 1} \right)$$

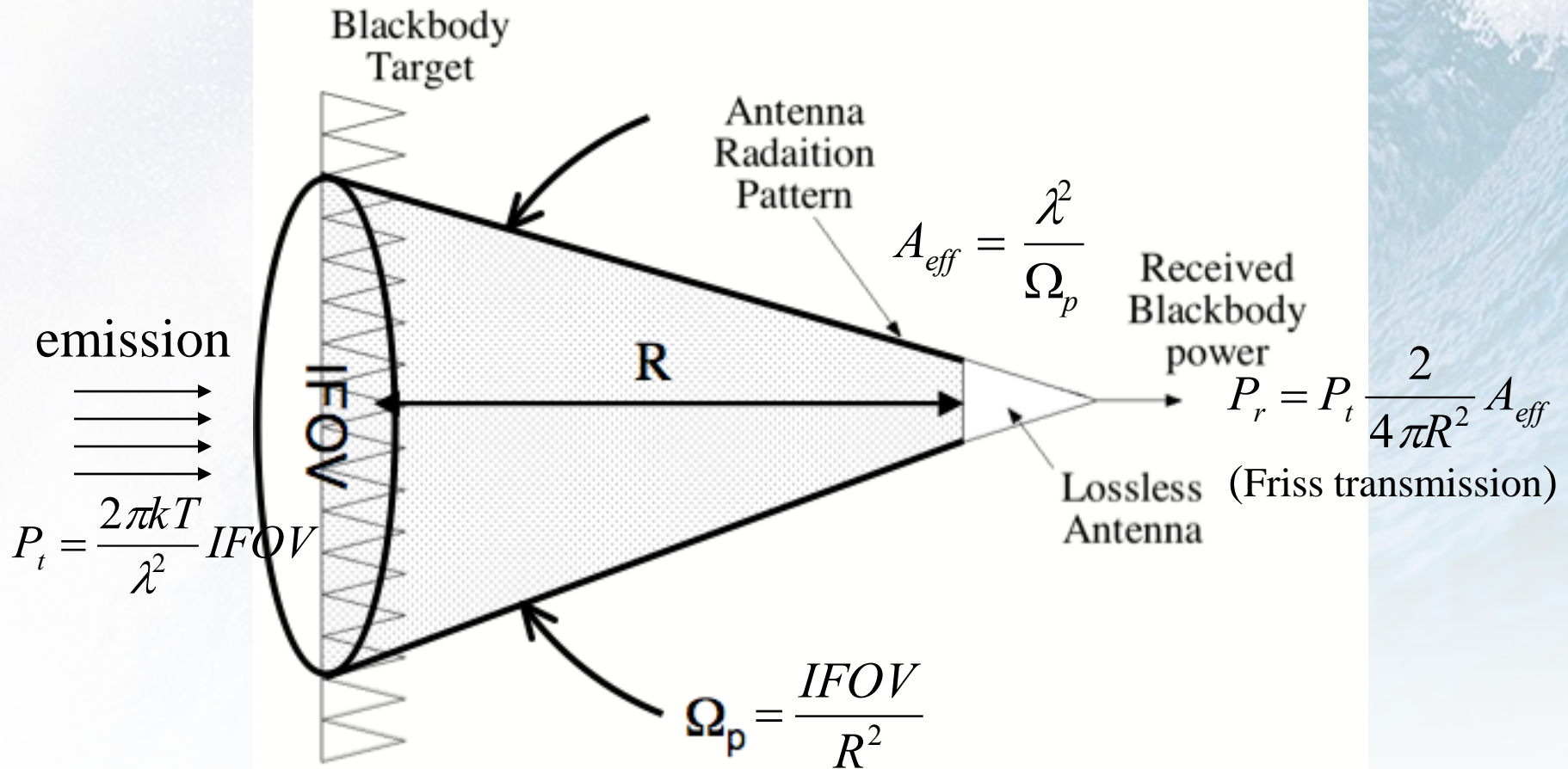
Given $hf/kT \ll 1$

$$e^{hf/kT} - 1 \approx hf/kT$$

$$S_f = \frac{2\pi f^2 kT}{c^2} = \frac{2\pi kT}{\lambda^2}$$

, Watts/ m^2/Hz

Radiometer Antenna



Radiometer received power

- Power density at the radiometer antenna

$$P_r = kT \quad , \text{Watts/Hz}$$

- Power received by the radiometer with system bandwidth B

$$P_r = kTB \quad , \text{Watts}$$

Brightness Temperature

- For non-blackbody, the equivalent radiometric blackbody temperature defined as

$$T_B = ET_{phy}$$

E = emissivity

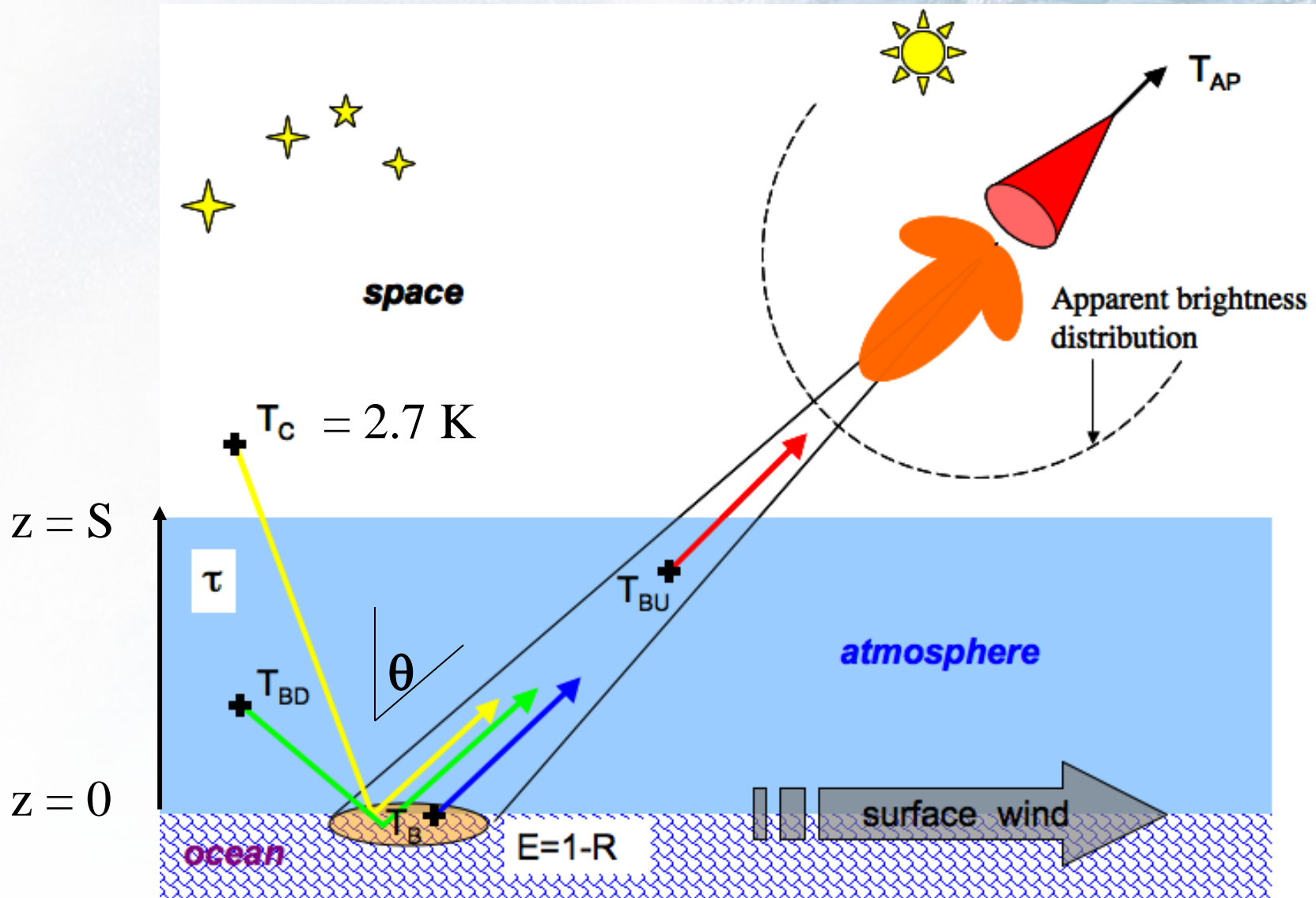
T_B = brightness temperature

T_{phy} = physical temperature of the target

- Received power becomes

$$P_r = kT_B B$$

Radiative Transfer Model (RTM)



Ocean Brightness Temperature

- Power emitted and reflected from ocean surface is strongly polarized
- Emissivity is depend of the air/sea boundary power reflection coefficient

$$E = 1 - R = 1 - |\rho|^2$$

$$\boxed{T_B = E \cdot SST}$$

SST = sea surface temperature

$$\rho_V = - \left(\frac{\epsilon_r \cos \theta - \sqrt{\epsilon_r - \sin^2 \theta}}{\epsilon_r \cos \theta + \sqrt{\epsilon_r - \sin^2 \theta}} \right)$$

$$\rho_H = - \left(\frac{\cos \theta - \sqrt{\epsilon_r - \sin^2 \theta}}{\cos \theta + \sqrt{\epsilon_r - \sin^2 \theta}} \right)$$

ϵ_r = dielectric constant
of sea water

Atmospheric brightness temp.

- Atmospheric emission is isotropic and non-polarized
- Emissivity characterize by atmospheric absorption coefficient, $\alpha(z)$, Neper/m (assume non-scattering)

$$T_{BU} = \int_0^{\infty} \alpha(z) T(z) \tau(z, S) dz$$
$$\tau(z_1, z_2) = \exp\left(-\int_{z_1}^{z_2} \alpha(z) dz\right)$$

$$T_{BD} = \int_0^{\infty} \alpha(z) T(z) \tau(0, z) dz$$

= atmospheric
transmissivity

$T(z)$ = atmospheric physical
temperature profile

Atmospheric brightness temp. -2

- Special case for homogeneous atmosphere

$$T(z) \approx T = \text{constant}$$

$$\alpha(z) \approx \alpha = \text{constant}$$

- Up-welling and down-welling brightness temp is approximated:

$$T_{BU} = T_{BD} \approx \int_0^S \alpha \cdot T \cdot e^{-\alpha \cdot z} dz = (1 - e^{-\alpha \cdot S})T$$

$$\tau = \tau(0, S) = e^{-\alpha \cdot S}$$

= total atmospheric
transmissivity

$$T_{BU} = T_{BD} \approx (1 - \tau)T$$

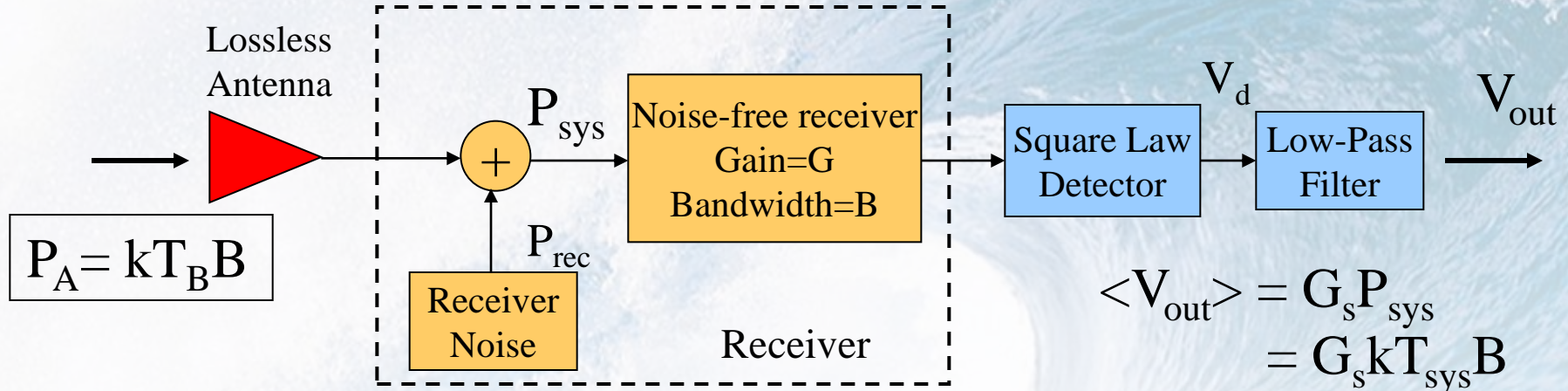
Apparent brightness temperature

- Total brightness temperature “seen” by radiometer antenna:

$$T_{AP} = \underbrace{T_{BU}}_{\text{upwelling component}} + \underbrace{\tau R(1 + \Omega)(T_{BD} + \tau T_g)}_{\text{scattering component}} + \underbrace{\tau E_2 S_3 T}_{\text{surface component}}$$

Ω = roughen surface scattering factor due to wind speed

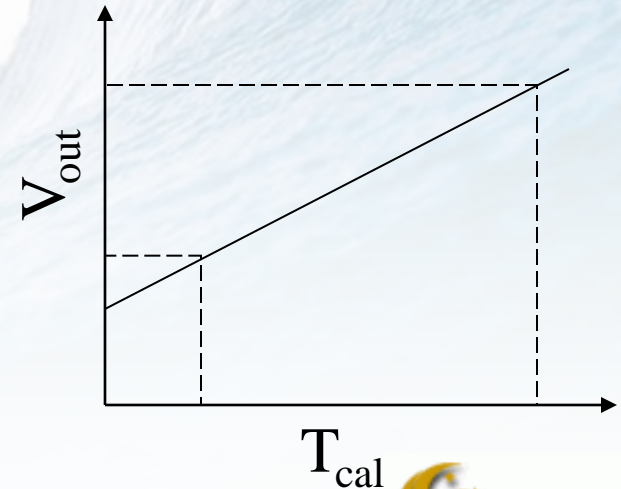
Radiometer System



$$P_{sys} = P_A + P_{rec} = kT_{sys} B$$

$$T_{sys} = T_B + T_{rec}$$

$$\Delta T_{sys} = \frac{T_{sys}}{\sqrt{B\tau}} = \text{measurement standard deviation}$$



Scatterometry

- Scatterometer is a radar instrument designed primarily to measure ocean vector wind (speed and direction)
- Backscatter signal is relatively insensitive to the atmosphere except for presence of rain
- Basic Radar Equation:

$$P_r = \frac{P_t G^2 \lambda^2}{(4\pi)^3 R^4} \sigma$$

σ = radar cross-section

$$\overline{P_r} = \frac{\lambda^2}{(4\pi)^3} \int \frac{P_t G^2 \sigma^0 dA}{R^4}$$

$$\sigma^0 = \left\langle \frac{\sigma_i}{\Delta A_i} \right\rangle = \text{normalized radar cross-section (NRSC)}$$

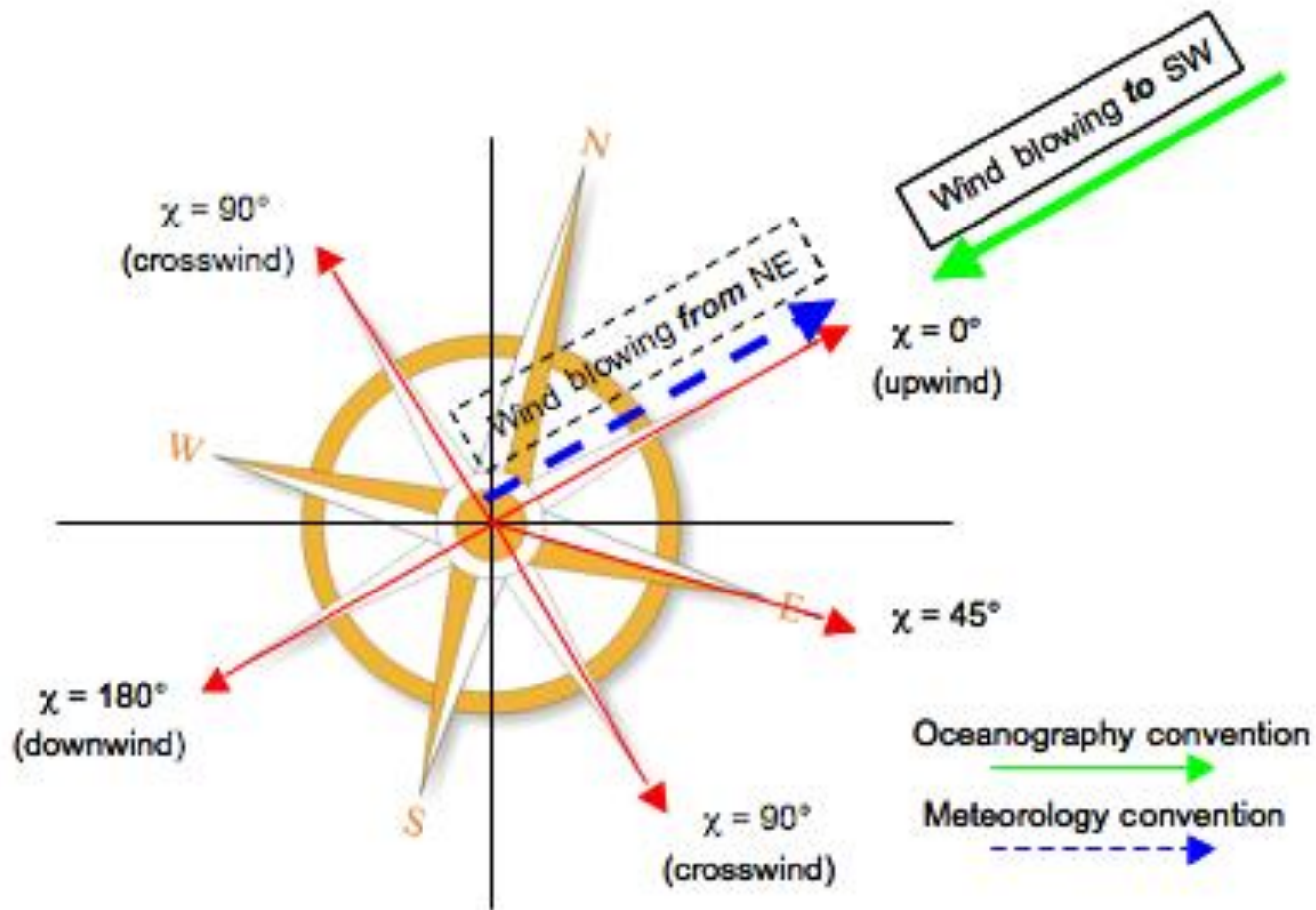
Geophysical Model Function

- Empirical relationship between σ^0 and wind vector is known as GMF
- GMF may be modeled as two harmonic cosine functions

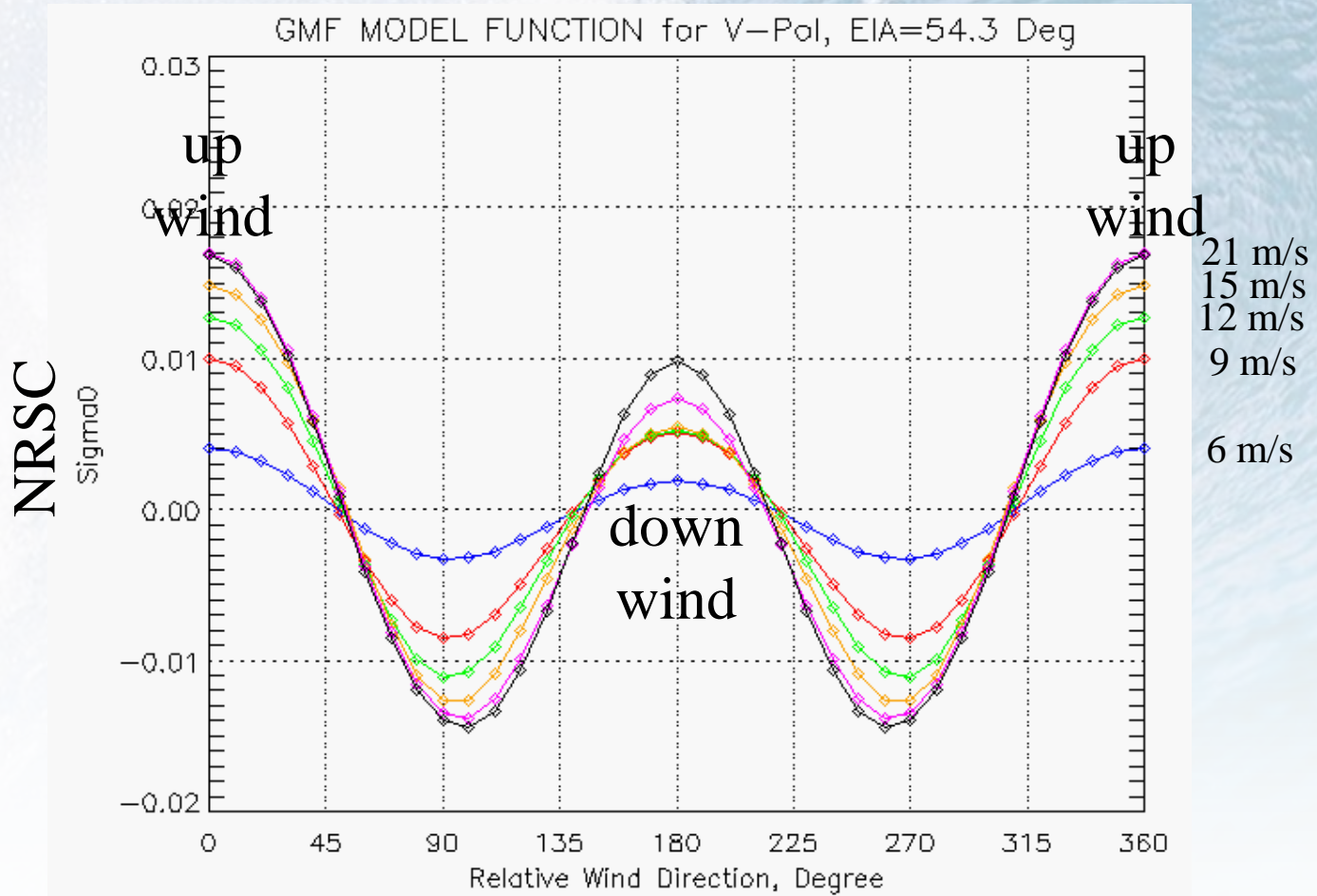
$$\sigma^0 = C_0(wspd) + C_1(wspd)\cos(\chi) + C_2(wspd)\cos(2\chi)$$

- GMF is also a function of incidence angle and observed polarization

Relative Wind Direction (χ)

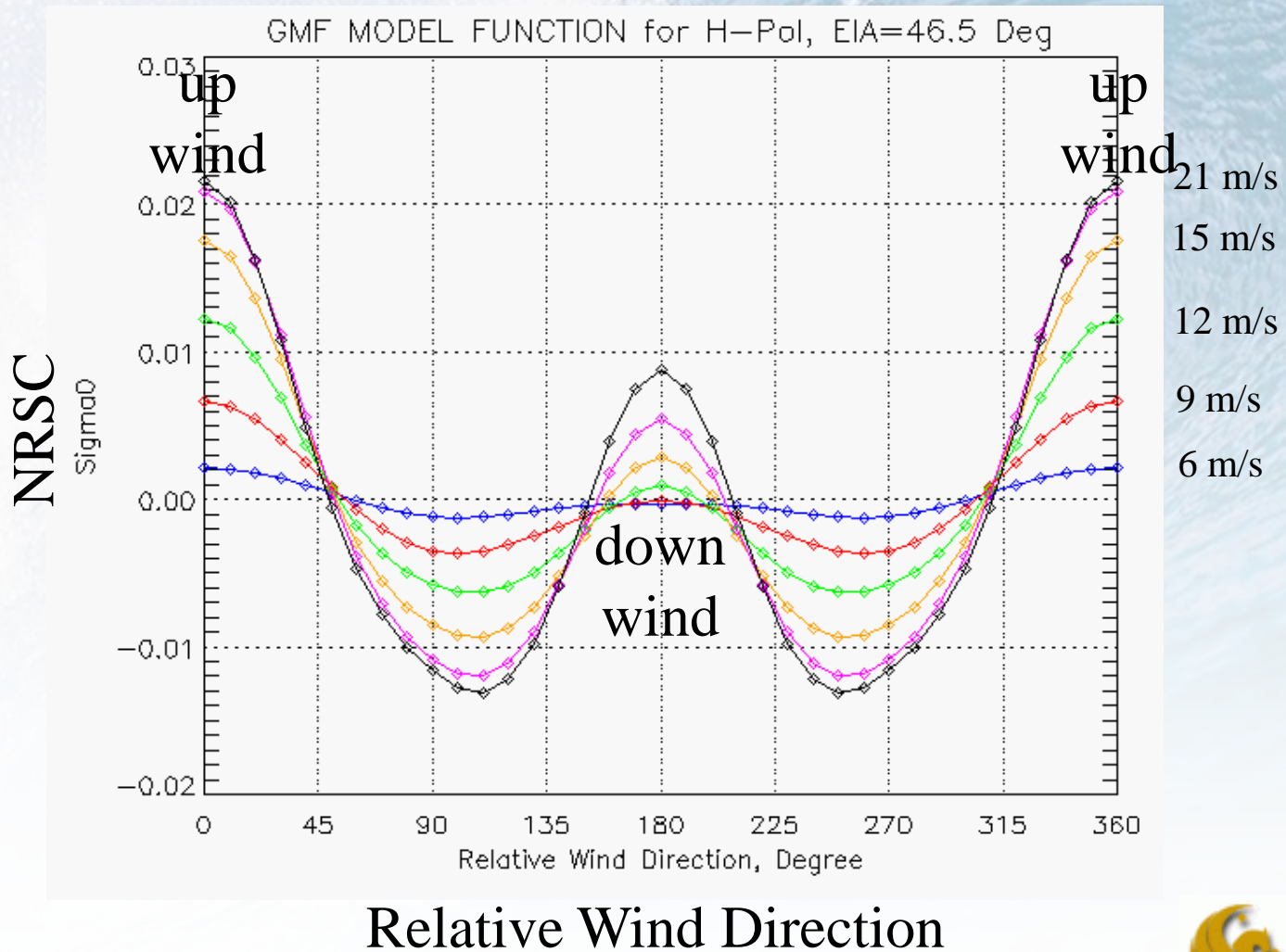


GMF for Scat V-Pol (C_o mean removed)



Relative Wind Direction

GMF for Scat H-Pol (C_0 mean removed)



Retrieval Algorithm

- Scatterometer requires backscatter measurements from multiple direction (fore and aft) to resolve wind direction
- Retrieval algorithm is based on maximum likelihood estimation (MLE)

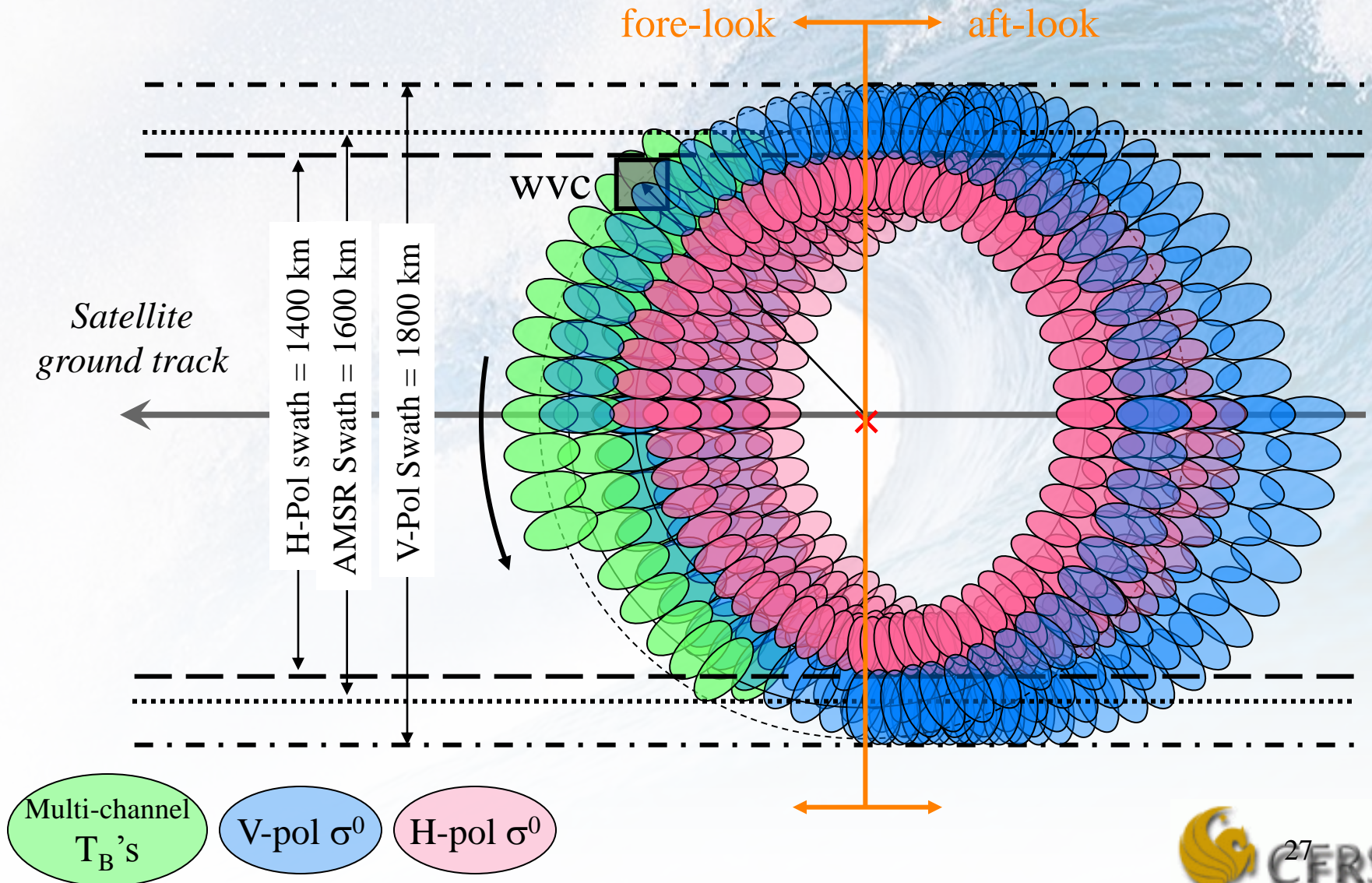
$$\zeta = \sum_i \frac{(\sigma_i^0 - GMF(wspd, \chi))^2}{Variance_{\sigma_i^0}(wspd, \chi)}$$

- Require nudging and median filtering to select a unique wind vector (known as direction ambiguity removal)

ADEOS-II Satellite

- AMSR
 - Dual-Polarization Multi-frequency:
6.9, 10.7, 18.7, 23.8,
36.5, 89.0 GHz
 - incidence angle: 55°
 - Integration time: 2.6 ms
 - Bandwidth:
100-3000 MHz
- SeaWinds
 - Dual-Polarization
13.4 GHz, 110 W, 189
PRF
 - incidence angle:
 54° V-pol,
 46° H-pol
 - 18 RPM
 - Bandwidth: 250 kHz

Measurement Geometry



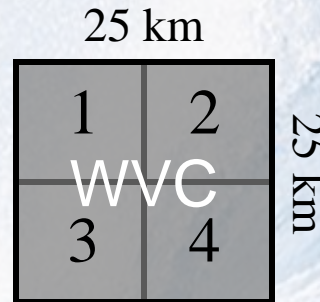
Satellite data product

- AMSR

- Overlay L2A product

- Brightness Temp. (T_B): 10, 18, 37 GHz

- Water vapor
- Cloud liquid water
- Rain
- SST



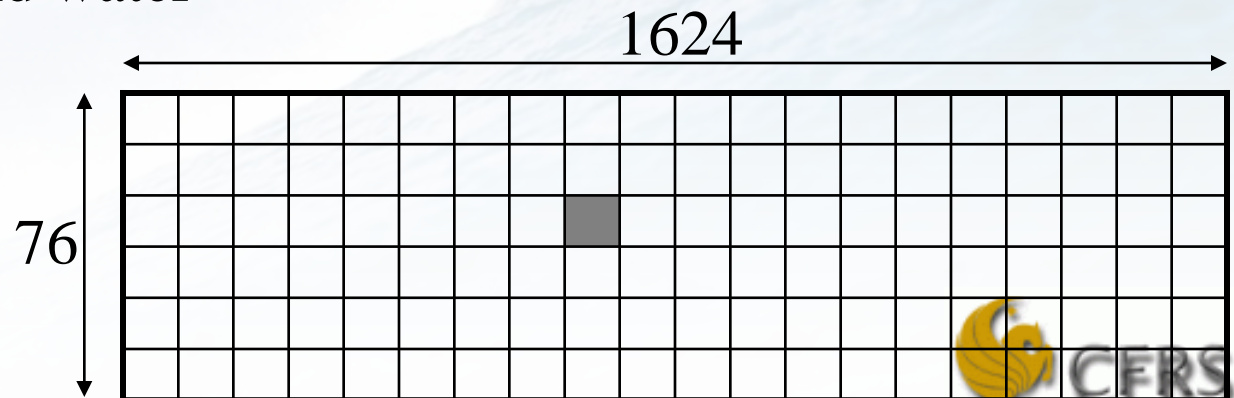
- SeaWinds

- L2A product

- Sigma-0

- L2B product

- Wind speed
- Wind direction



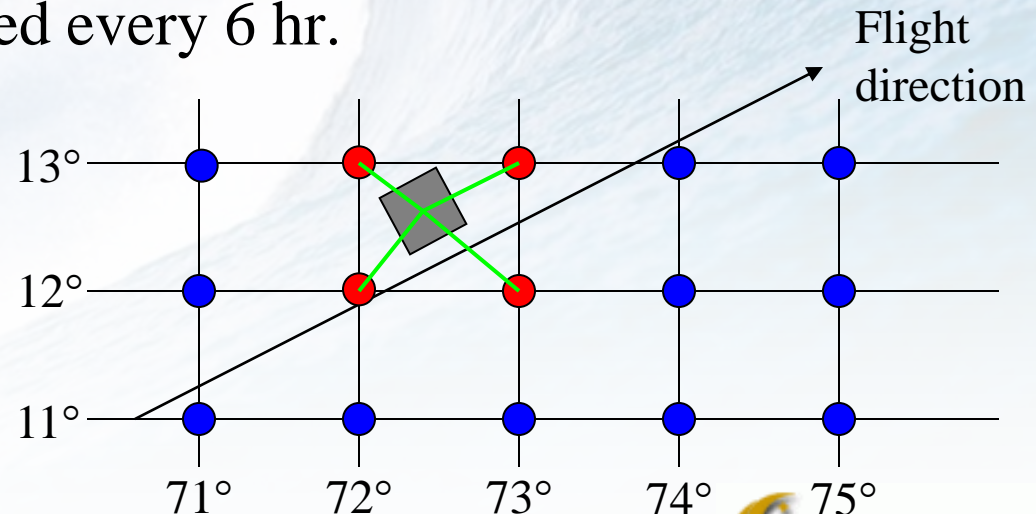
Other required data

- AMSR azimuth

- Calculated from AMSR measurement geometry, scan radius (940 km) with WVC location

- Sea surface temperature (SST)

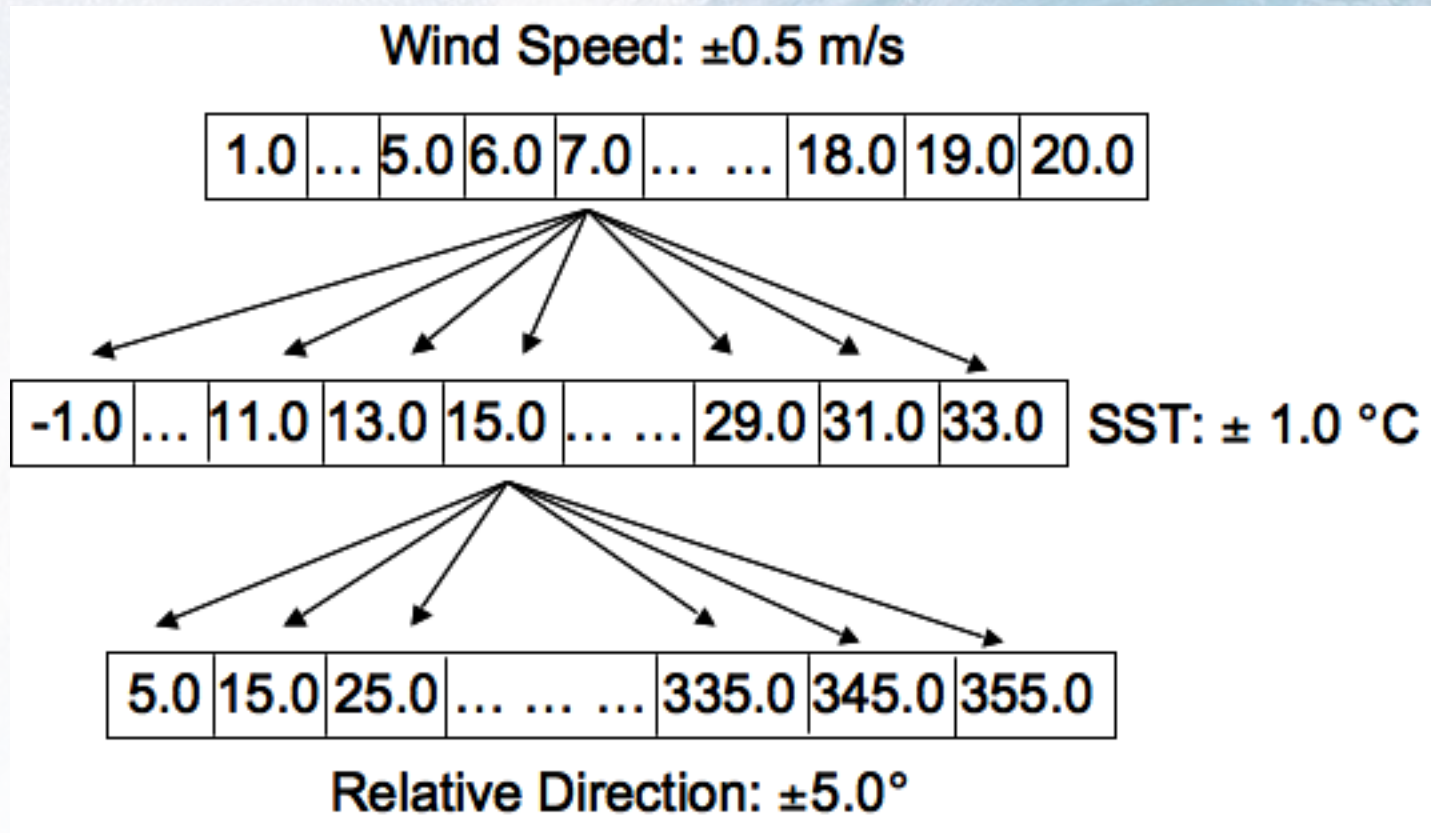
- NCEP's Global Data Assimilation System (GDAS)
 - Global map generated every 6 hr.
 - $1^\circ \times 1^\circ$ resolution



Data Match-Ups

- AMSR and SeaWinds data were automatically collocated
- GDAS's SST match-up required additional work
 - Four point interpolation surrounding AMSR WVC's quadrants
- Average AMSR parameters into single WVC's
- All data were match-up over entire mission period of Apr - Oct, 2003
- Filtered out rain and high cloud liquid water (<0.1mm)

Binned Data Scheme



RTM Assumption

- Atmosphere is homogeneous: Temp. profile and absorption is constant

$$T_{BU} = T_{BD} = (1 - \tau)T$$

- Air/Sea temperature is the same: Effective temperature

$$T = SST = T_{eff}$$

$$T_{BU} = T_{BD} = (1 - \tau)T_{eff}$$

RTM Assumption -2

$$T_{AP} = \underbrace{T_{BU}}_{\text{upwelling component}} + \underbrace{\tau R(1 + \Omega)(T_{BD} + \tau T_C)}_{\text{scattering component}} + \underbrace{\tau E \cdot SST}_{\text{surface component}}$$

$$\text{upwelling} = T_{BU} = (1 - \tau)T_{eff} = T_{eff} - \cancel{\tau T_{eff}}$$

$$\begin{aligned} \text{scattering} &= \tau R T_{BD} + \tau R \Omega T_{BD} + \tau^2 R(1 + \Omega)T_C \\ &= \tau R(1 - \tau)T_{eff} + \tau R \Omega(1 - \tau)T_{eff} + \tau^2 R(1 + \Omega)T_C \\ &= \cancel{\tau R T_{eff}} - \tau^2 R T_{eff} + \tau R \Omega(1 - \tau)T_{eff} + \tau^2 R(1 + \Omega)T_C \end{aligned}$$

$$\text{surface} = \tau E \cdot SST = \tau(1 - R) \cdot T_{eff} = \cancel{\tau T_{eff}} - \cancel{\tau R T_{eff}} \quad \text{negligible}$$

$$T_{AP} = T_{eff} - R\tau^2 T_{eff} + \cancel{R\tau\Omega(1 - \tau)T_{eff}} + \cancel{R\tau^2(1 + \Omega)T_C}$$

$$T_{AP} \approx (1 - R\tau^2) \cdot T_{eff}$$

Atmospheric cancellation

- The brightness temperature for vertical and horizontal polarization may be represented as:

$$T_{BV} = (1 - R_V \tau^2) T_{eff}$$

$$T_{BH} = (1 - R_H \tau^2) T_{eff}$$

- Define a new parameter, A as a ratio of V and H-pol

$$A \equiv \frac{R_H}{R_V}$$

- Changes in brightness temperature with respect to atmospheric transmissivity

$$\partial T_{BV} = -2R_V \tau T_{eff} \partial \tau$$

$$\partial T_{BH} = -2AR_V \tau T_{eff} \partial \tau$$

$$\frac{\partial (AT_{BV} - T_{BH})}{\partial \tau} = 0$$

“A” Parameter

- Linear combination of V and H brightness temperature is independent of atmosphere

$$\boxed{AT_{BV} - T_{BH}}$$

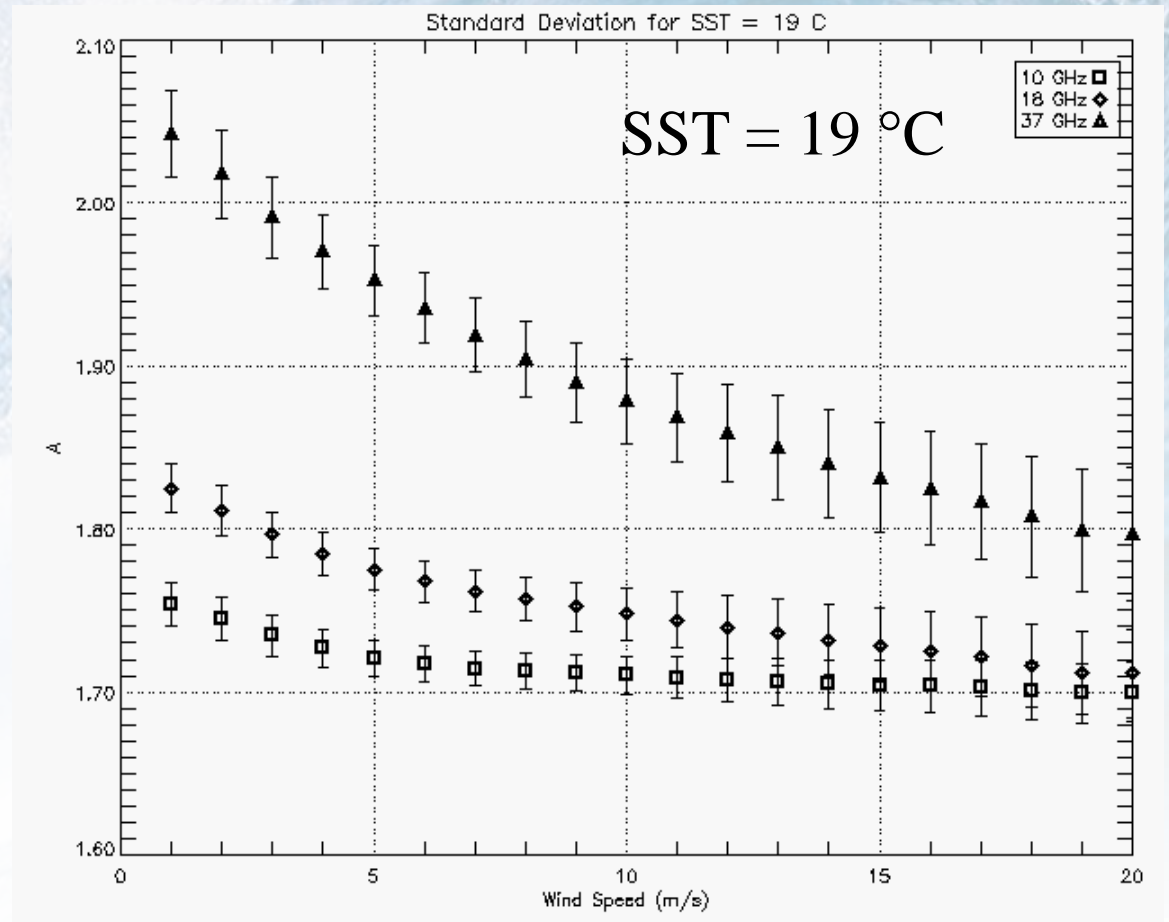
$$\begin{aligned} AT_{BV} - T_{BH} &= A(1 - R_V \tau^2)T_{eff} - (1 - R_H \tau^2)T_{eff} \\ &= (A - 1)T_{eff} - (\cancel{AR_V} - R_H)\tau^2 T_{eff} \end{aligned}$$

$$\boxed{A = \frac{T_{BH} - T_{eff}}{T_{BV} - T_{eff}}}$$

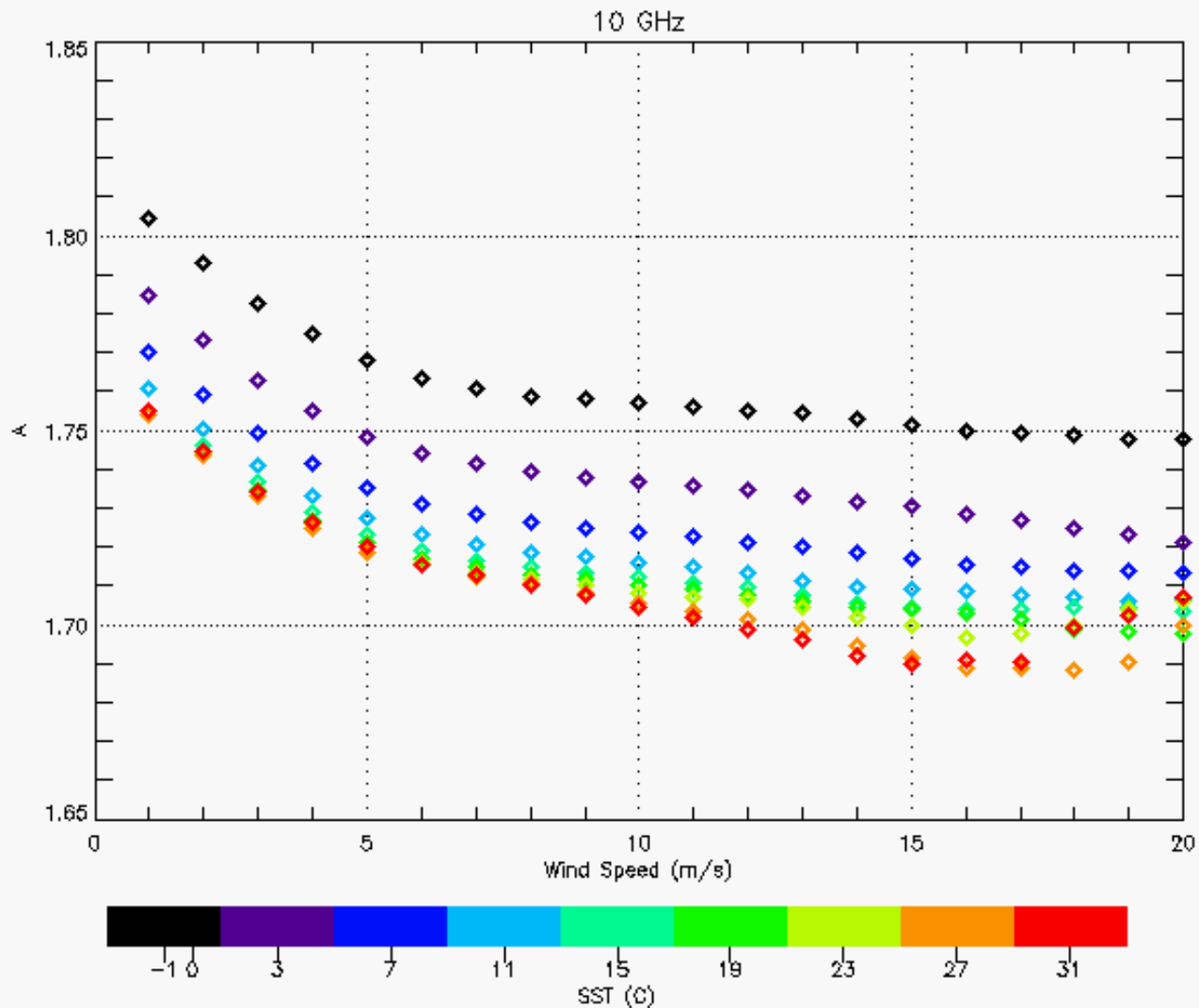
$$T_{eff} = SST$$

“A” Parameter -2

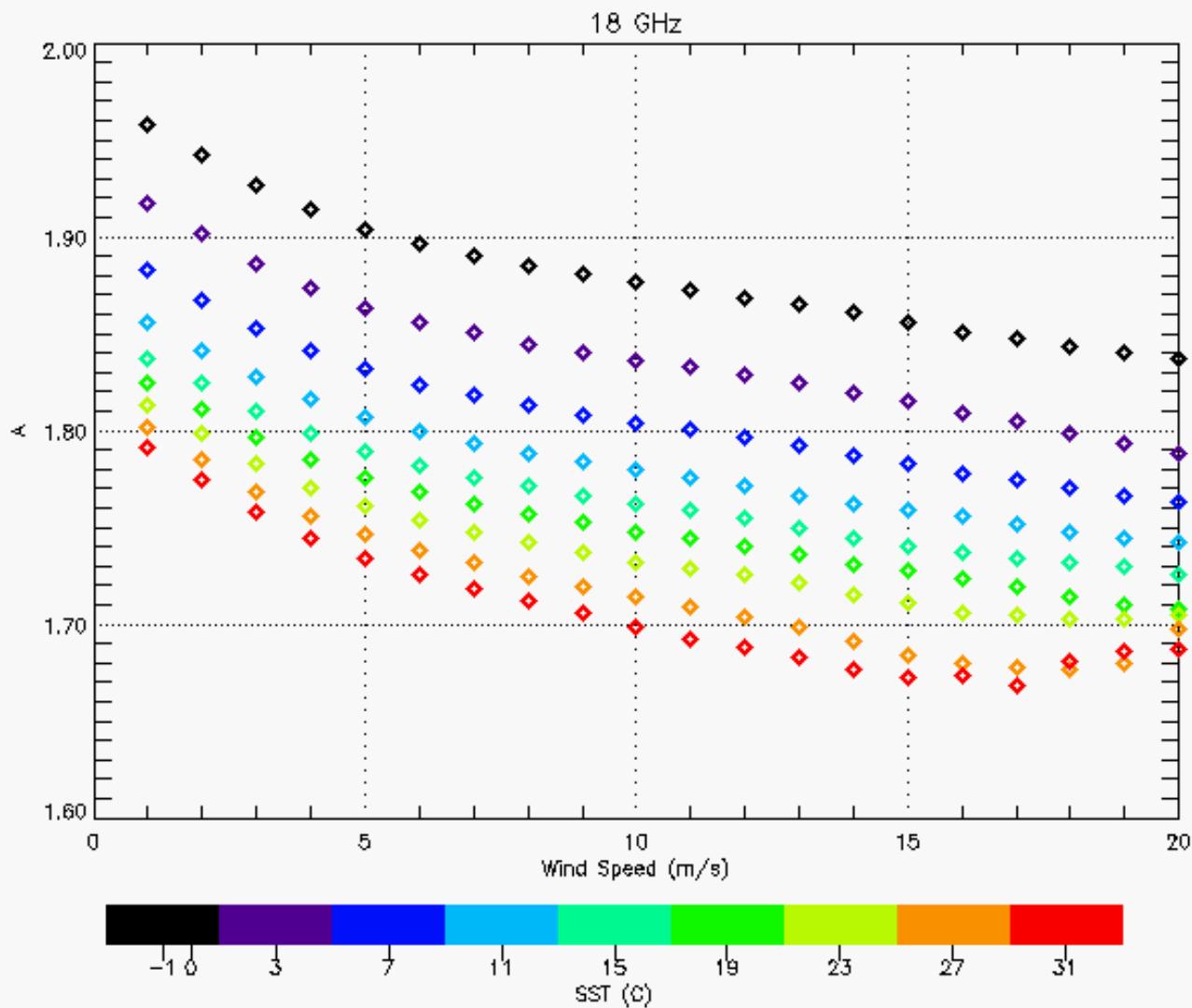
- A parameter has Gaussian distribution
- A was found as a function of wind speed (wspd) and sea surface temperature (SST)



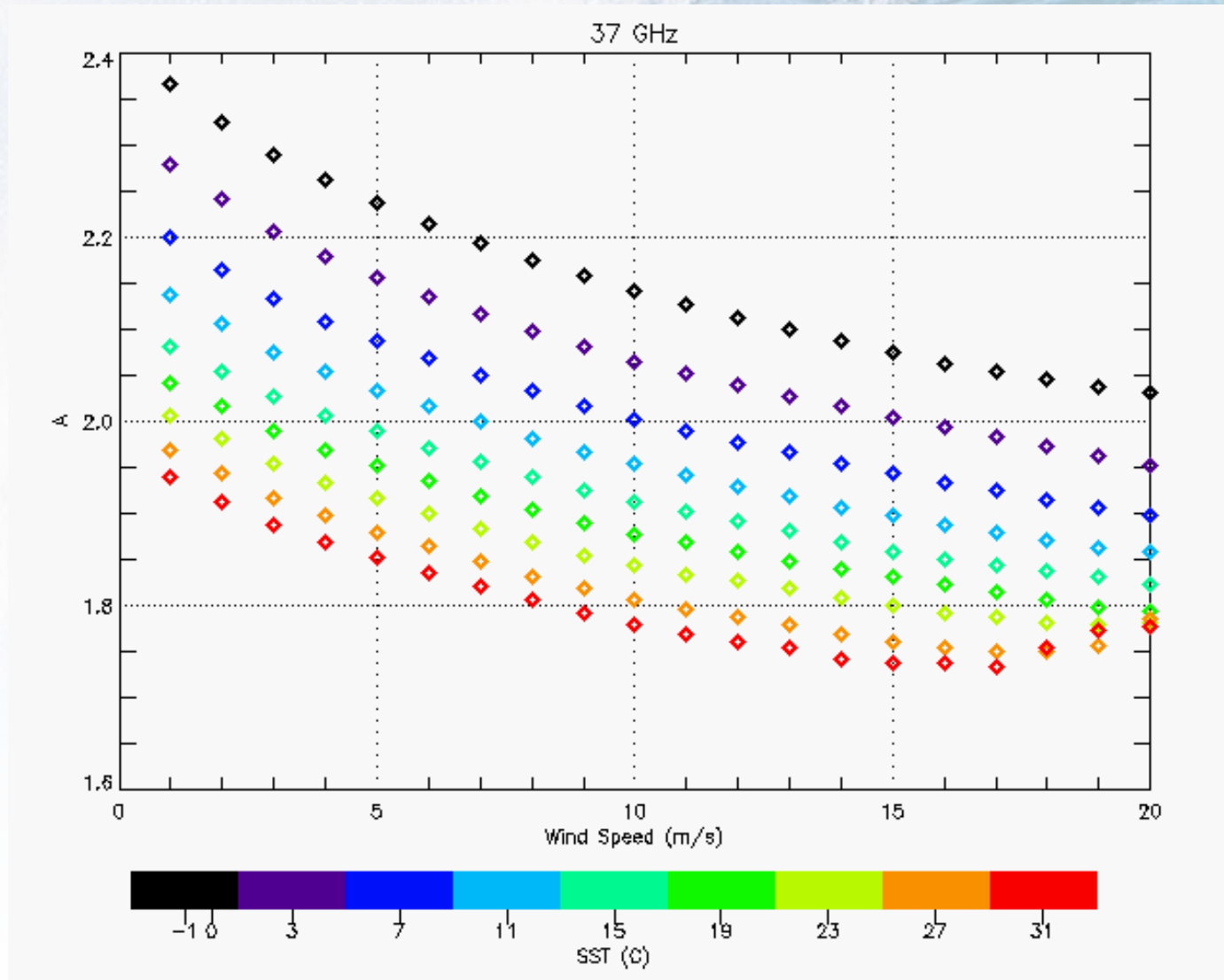
A parameter for 10 GHz



A parameter for 18 GHz



A parameter for 37 GHz



Model Function Procedure

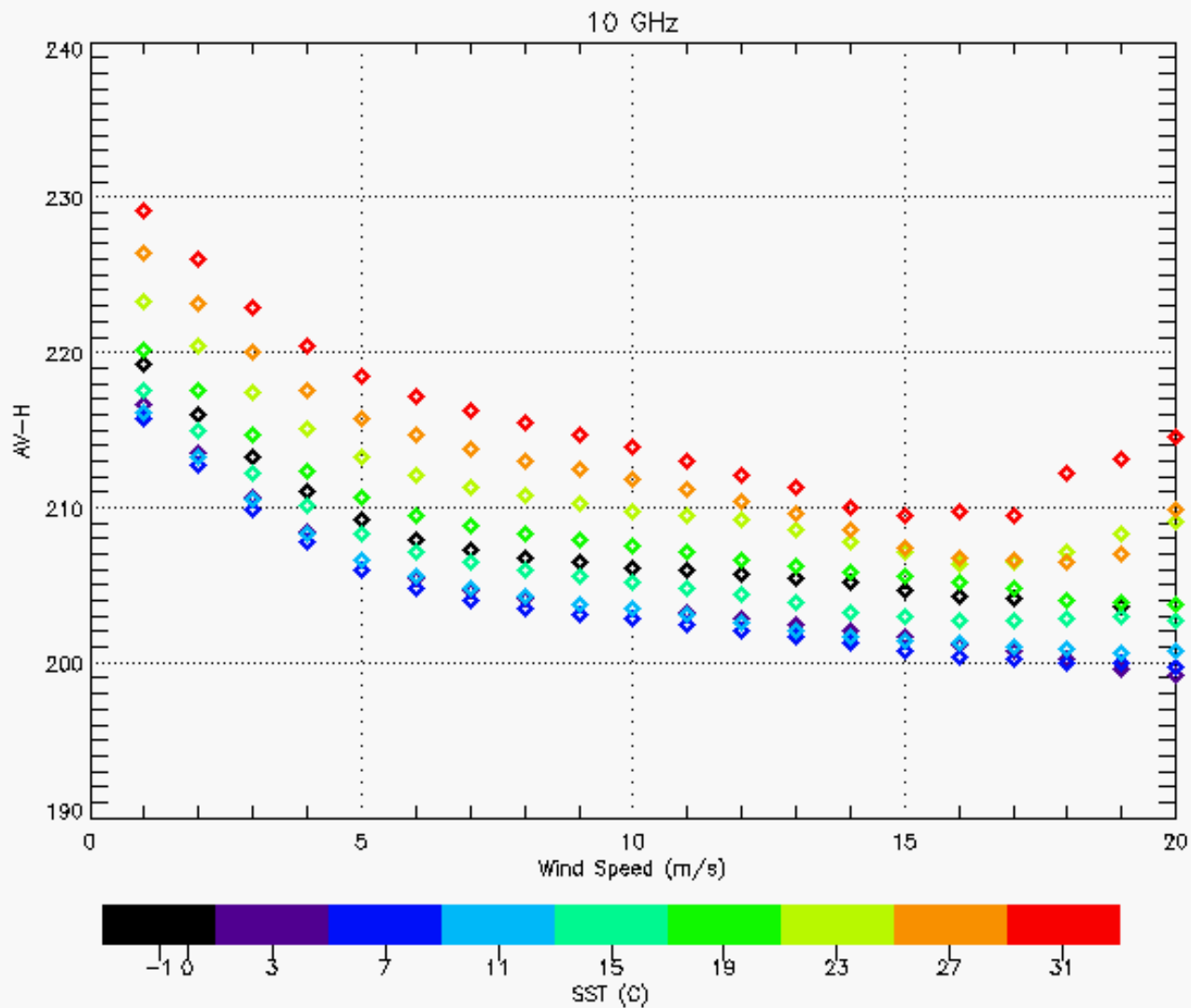
- $AT_{BV} - T_{BH}$ (AV-H) was found as a function of wind speed, wind direction and SST
- AV-H is model as a linear sum of each components

$$AT_{BV} - T_{BH} = F(SST) + C_0(WSPD) + C_1(WSPD) \cdot \cos(\chi) + C_2(WSPD) \cdot \cos(2\chi)$$

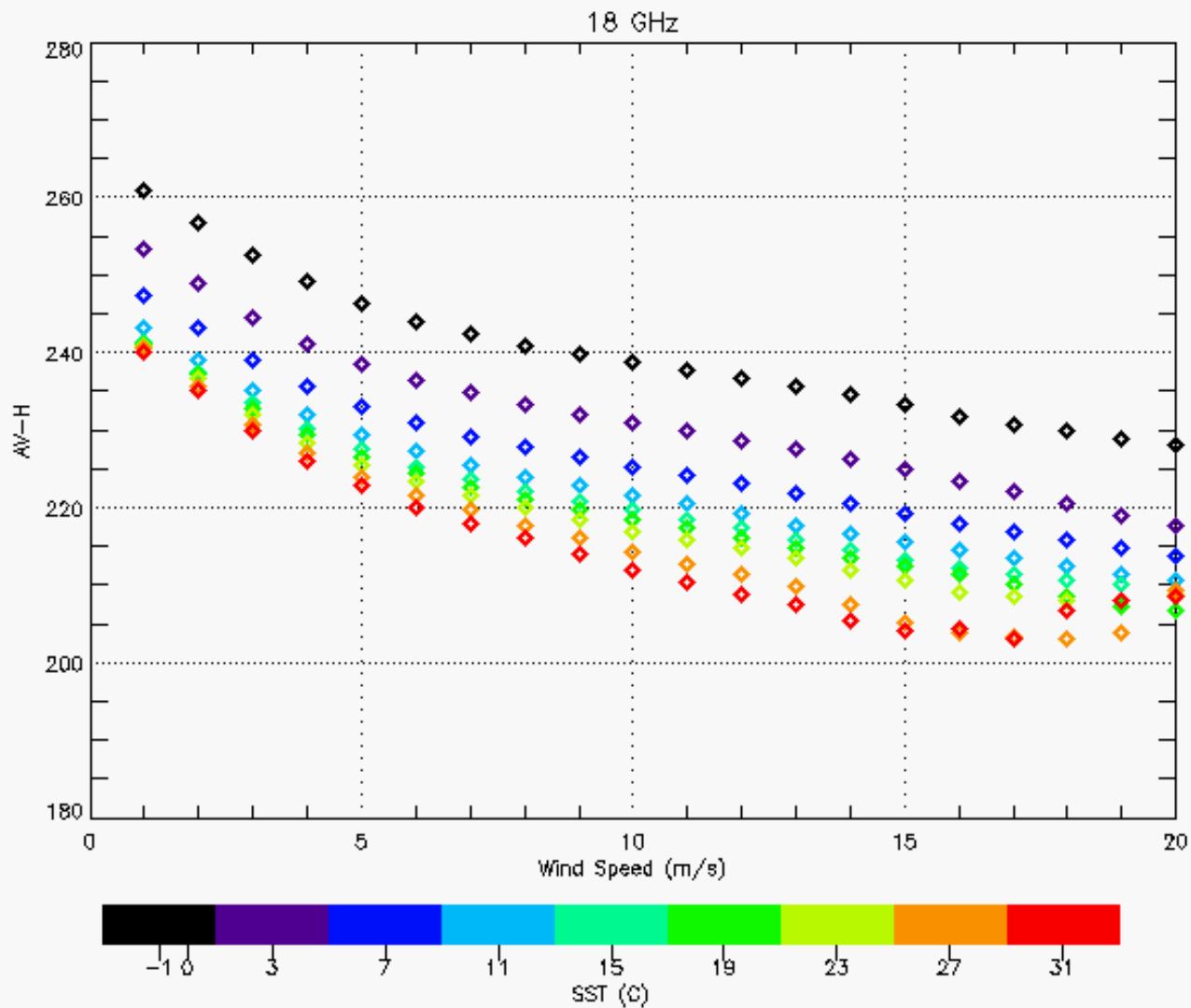
- Wind directional signal modeled as two harmonic cosine function

$$F(WDIR) = C_0(WSPD) + C_1(WSPD) \cdot \cos(\chi) + C_2(WSPD) \cdot \cos(2\chi)$$

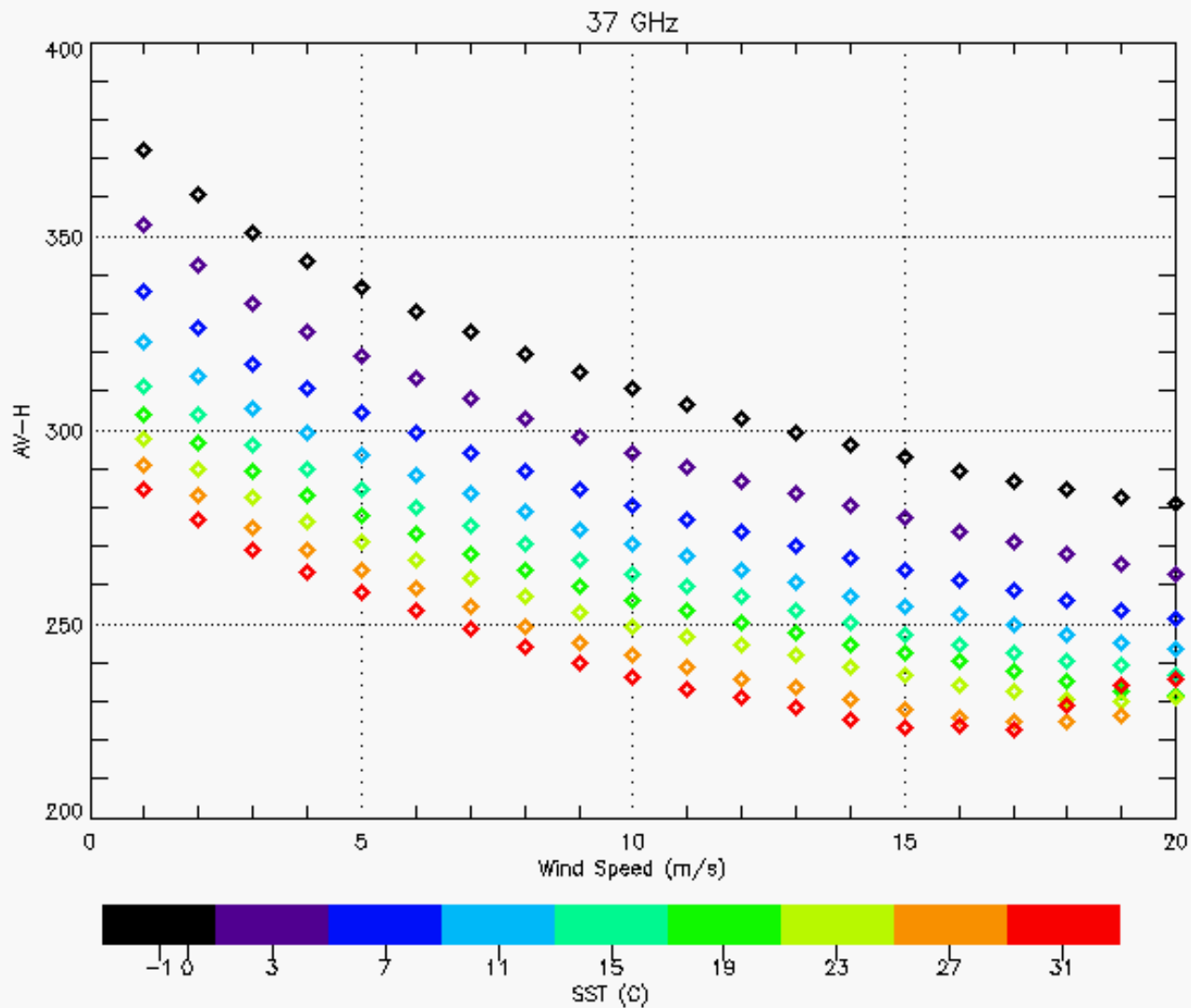
AV-H for 10 GHz



AV-H for 18 GHz



AV-H for 37 GHz



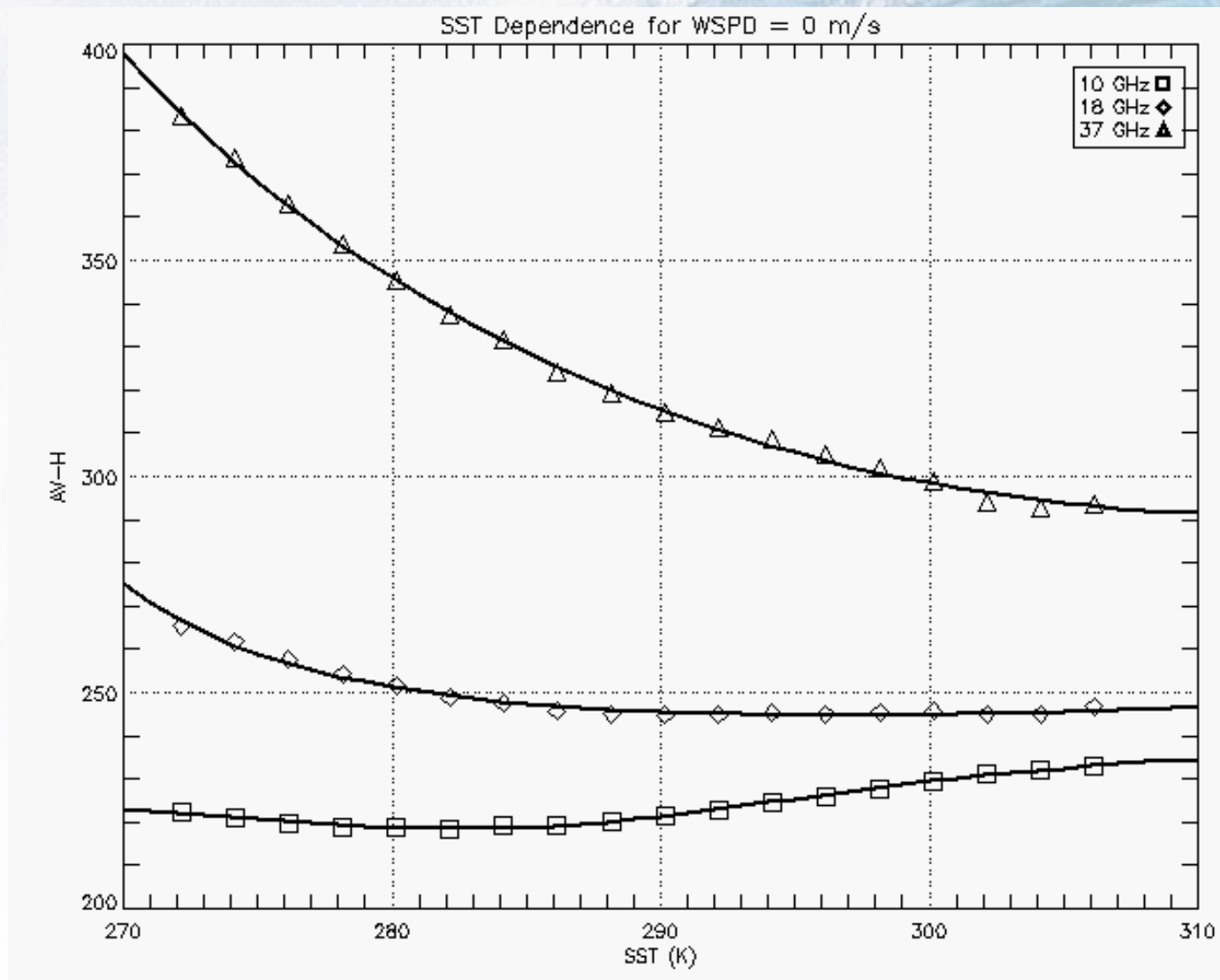
Procedure -2

- Assume sea surface is smooth: wind speed = 0 m/s
- AV-H become a function of only SST

$$AT_{BV} - T_{BH} = F(SST) + C_0(\cancel{WSPD})^0 + C_1(\cancel{WSPD})^0 \cdot \cos(\chi) + C_2(\cancel{WSPD})^0 \cdot \cos(2\chi)$$

- This initial $F(SST)$ found from extrapolation to zero wind speed values
- Appropriate function that best describes the measurement is found

Initial $F(SST)$



Procedure -3

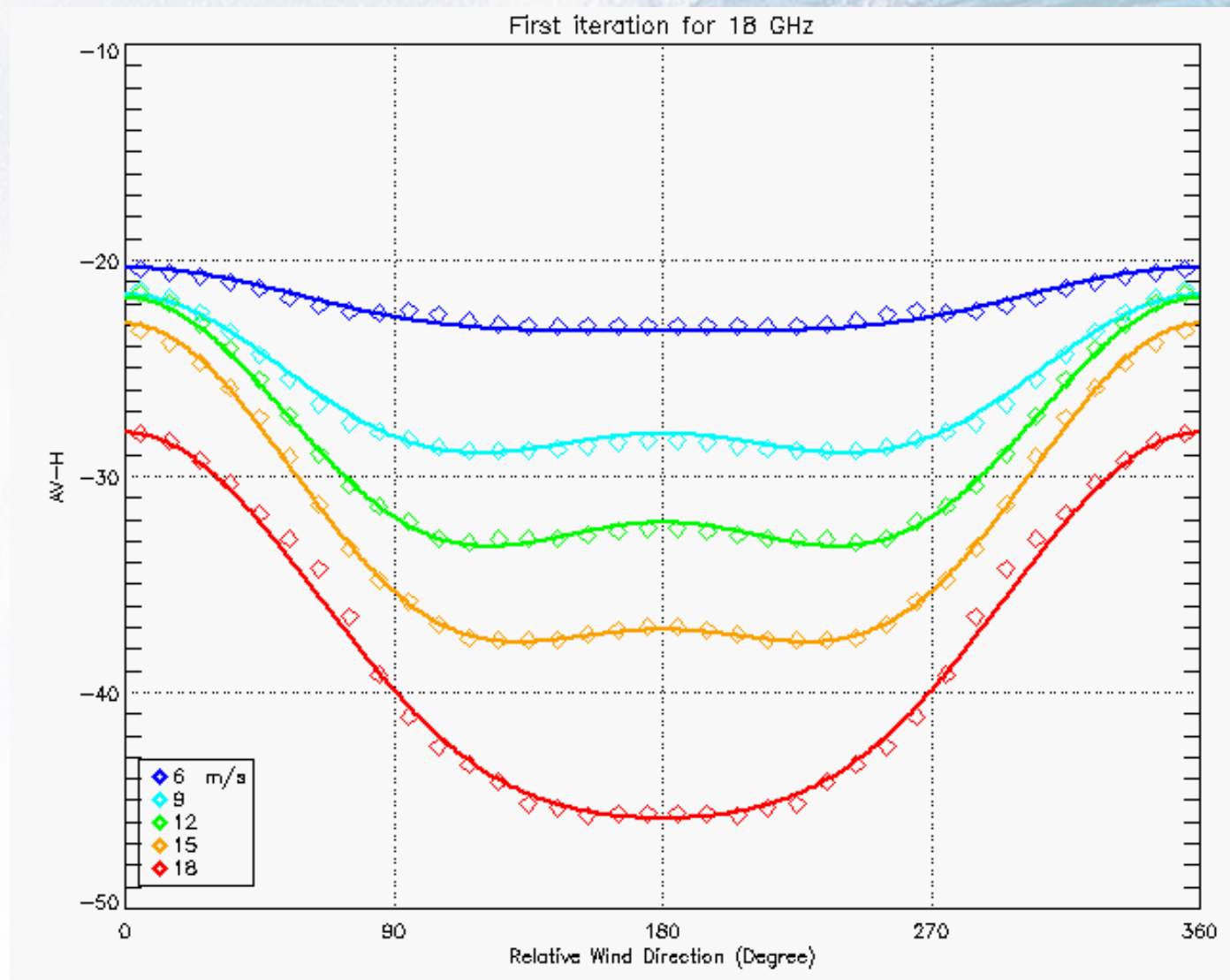
- Subtract $AV-H$ from initial $F(SST)$.
- Remaining $AV-H$ become a function of wind speed and direction

$$(AV - H) - F(SST) = F(WDIR)$$

- Find regression to the measurement in the form:

$$F(WDIR) = C_0(WSPD) + C_1(WSPD) \cdot \cos(\chi) + C_2(WSPD) \cdot \cos(2\chi)$$

First iteration $F(WDIR)$



Procedure -4

- The C 's coefficient was found for discrete values of wind speed bin
- Regression fit was found for each of the C 's coefficient. $F(WDIR)$ is found for all wind speed values.
- Iterative process has established

$$(AV - H) - F(WDIR) = F(SST)$$

Model Equations

$$AT_{BV} - T_{BH} = F(SST) + C_0(WSPD) + C_1(WSPD) \cdot \cos(\chi) + C_2(WSPD) \cdot \cos(2\chi)$$

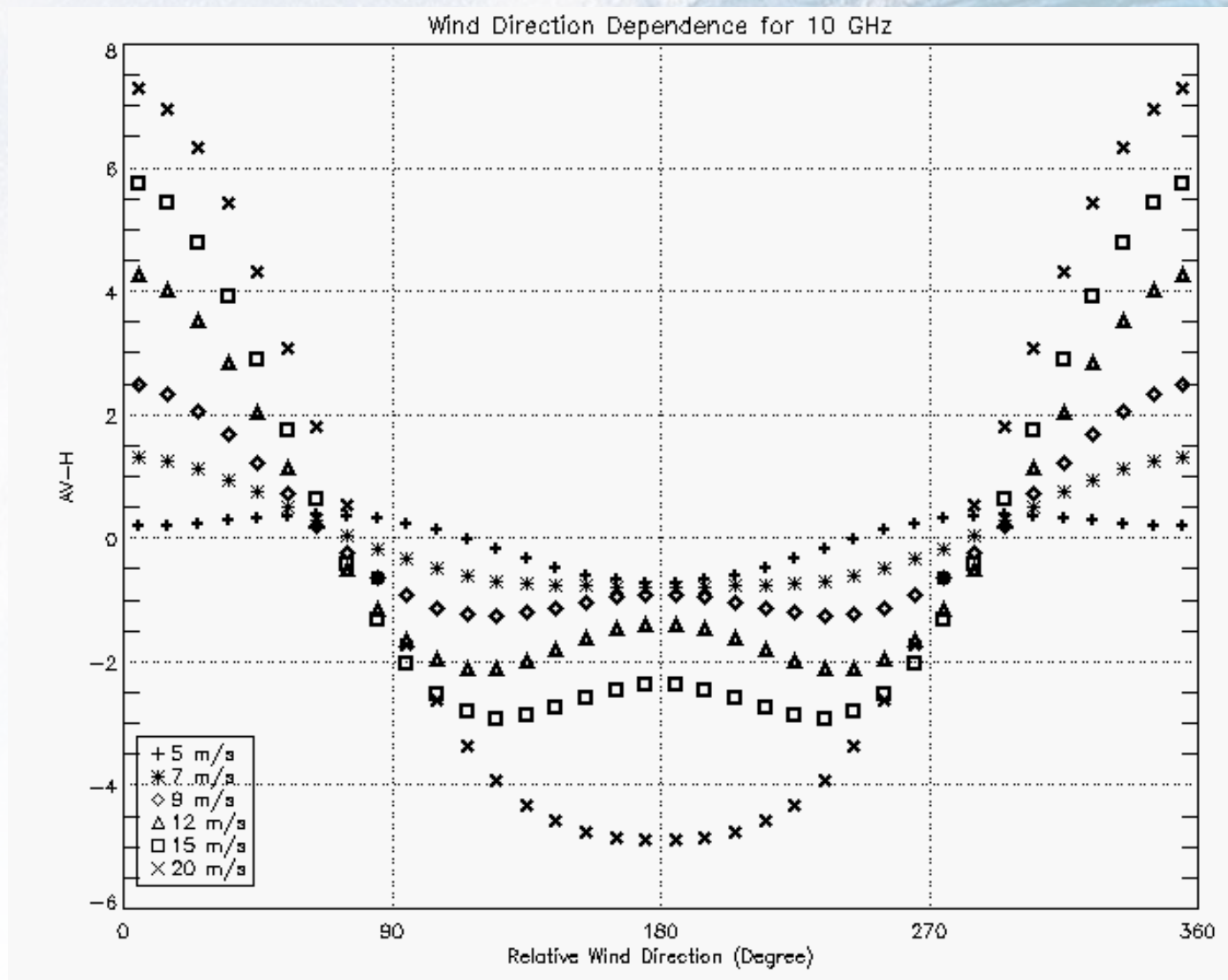
		F(SST)	C ₀ (WSPD)	C ₁ (WSPD)	C ₂ (WSPD)
AMSR Channel	10 GHz	$\frac{a+c \cdot x+e \cdot x^{2**}}{1+b \cdot x+d \cdot x^2}$	$\frac{a+c \cdot x+e \cdot x^2+g \cdot x^3}{1+b \cdot x+d \cdot x^2+f \cdot x^3}$	$\frac{a+c \cdot x}{1+b \cdot x+d \cdot x^2}^*$	$\frac{a+c \cdot x+e \cdot x^{2*}}{1+b \cdot x+d \cdot x^2}$
	18 GHz	$\frac{a+c \cdot x^{**}}{1+b \cdot x}$	$\frac{a+c \cdot x+e \cdot x^2+g \cdot x^3}{1+b \cdot x+d \cdot x^2+f \cdot x^3}$	$\frac{a+c \cdot x}{1+b \cdot x+d \cdot x^2}^*$	$\frac{a+c \cdot x+e \cdot x^{2*}}{1+b \cdot x+d \cdot x^2}$
	37 GHz	$\frac{a+c \cdot x^{**}}{1+b \cdot x}$	$\frac{a+c \cdot x+e \cdot x^2+g \cdot x^3}{1+b \cdot x+d \cdot x^2+f \cdot x^3}$	$\frac{a+c \cdot x}{1+b \cdot x+d \cdot x^2}^*$	$\frac{a+c \cdot x+e \cdot x^{2*}}{1+b \cdot x+d \cdot x^2}$

* First four points was excluded. ** Last point was excluded.

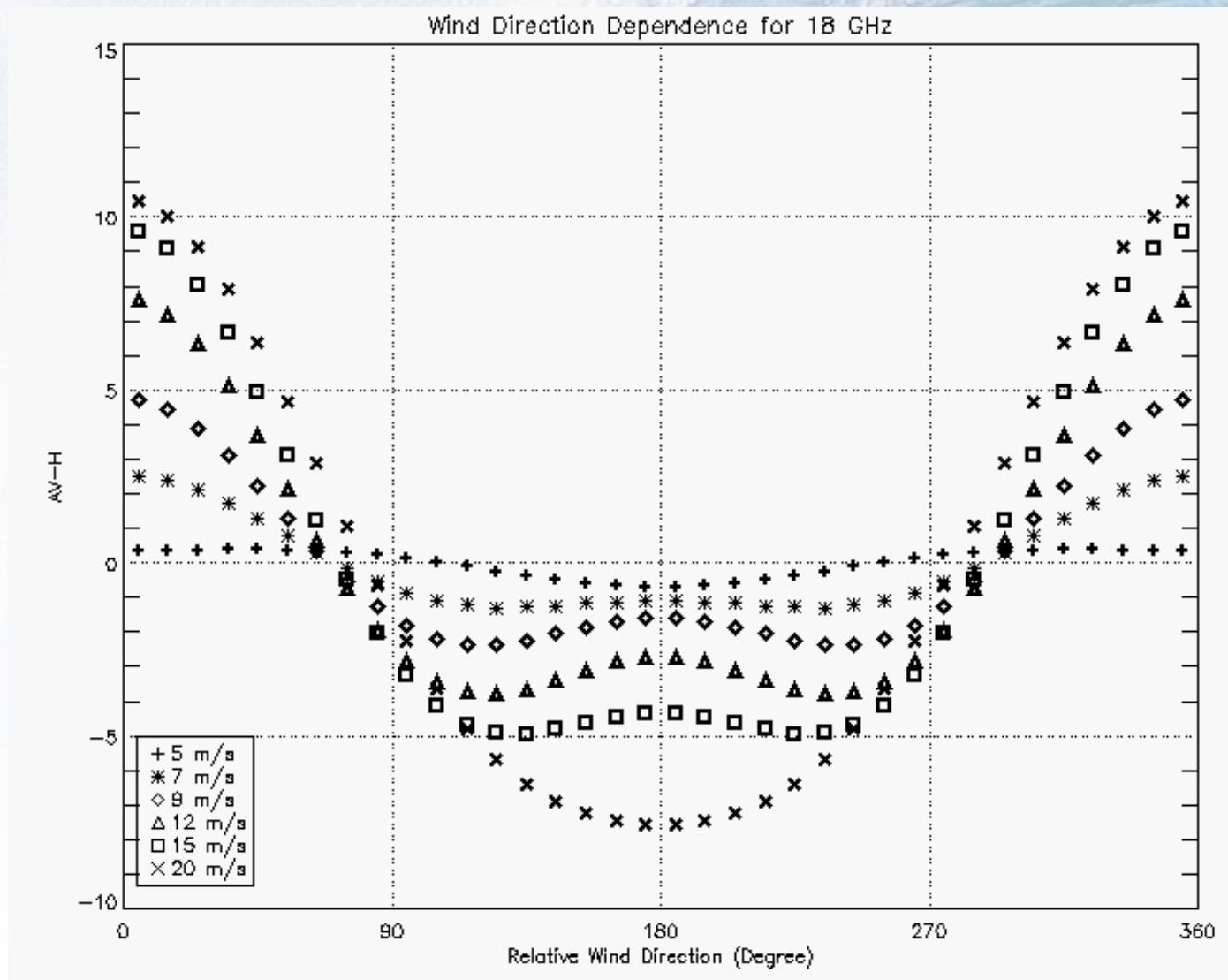
Model Coefficients

		F(SST)	C ₀ (WSPD)	C ₁ (WSPD)	C ₂ (WSPD)
AMSR Channels	10 GHz	a= 253.8939018 b= -0.007207942 c= -1.827465510 d= 1.3108e-05 e= 0.003314763	a= 0.517115747 b= -0.140174737 c= -3.734401755 d= 0.003843883 e= 0.787061774 f= 0.003616502 g= -0.101162061	a= -0.653431016 b= -0.042740230 c= 0.205632786 d= 0.001052848	a= -1.395843862 b= -0.073649495 c= 0.283917140 d= 0.002780937 e= -0.008776347
	18 GHz	a= 234.5302360 b= -0.003810786 c= -0.898157560	a= -0.268136601 b= -0.110325789 c= -3.522010565 d= 0.043939984 e= -0.167645682 f= 0.000277041 g= -0.075276385	a= -2.095456244 b= -0.039566361 c= 0.508449429 d= 0.001709247	a= -2.2041331797 b= -0.068904176 c= 0.501358865 d= 0.002615589 e= -0.017071887
	37 GHz	a= 193.3863684 b= -0.004205115 c= -0.907046083	a= 3.246690433 b= 0.139539136 c= -13.19966520 d= -0.006413733 e= 0.318536521 f= 0.000286851 g= -0.022678385	a= -5.056542254 b= -0.008215836 c= 1.147747275 d= 0.001194255	a= -2.019721861 b= -0.086047248 c= 0.430587232 d= 0.002842379 e= -0.015823182

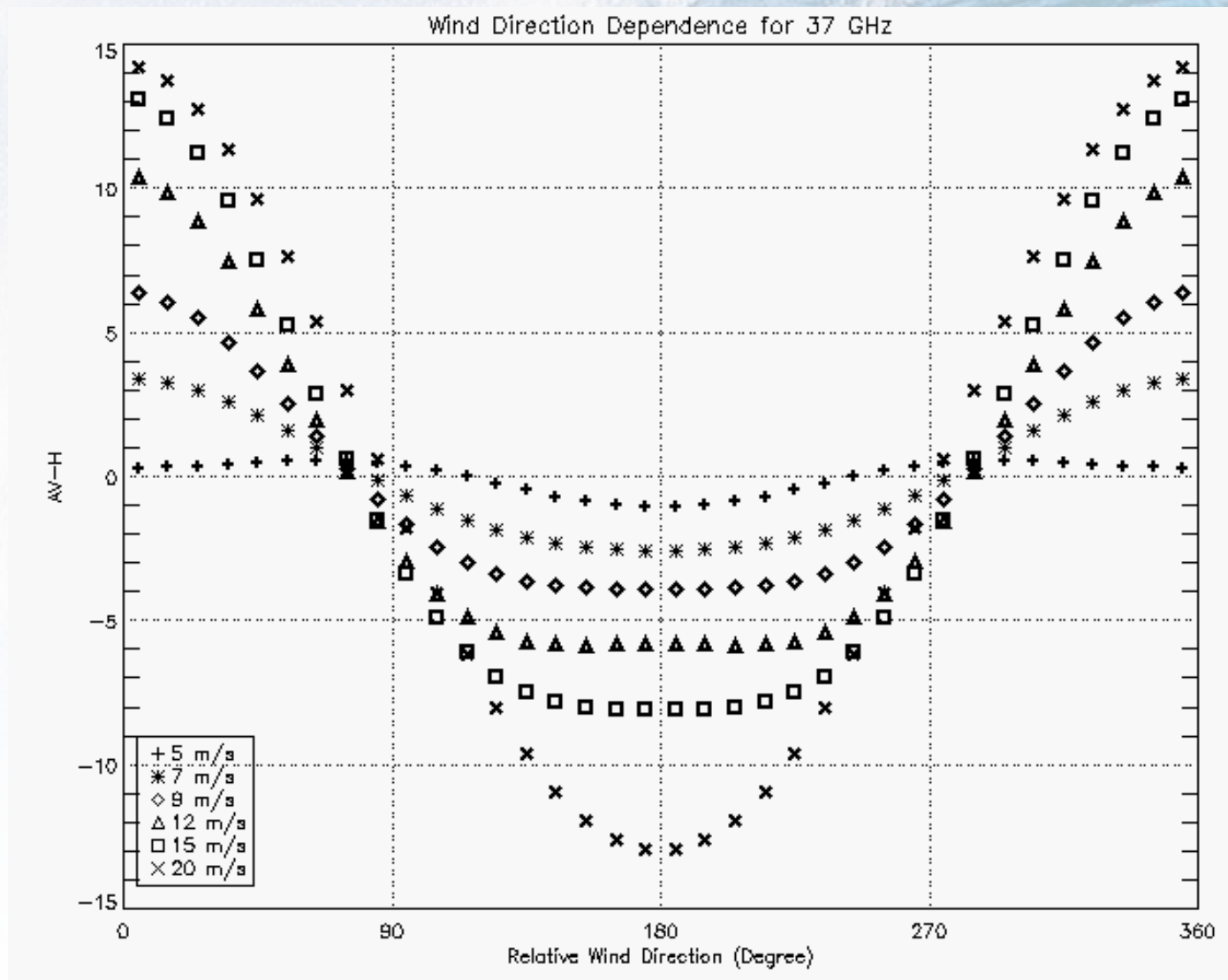
Model Function for 10 GHz



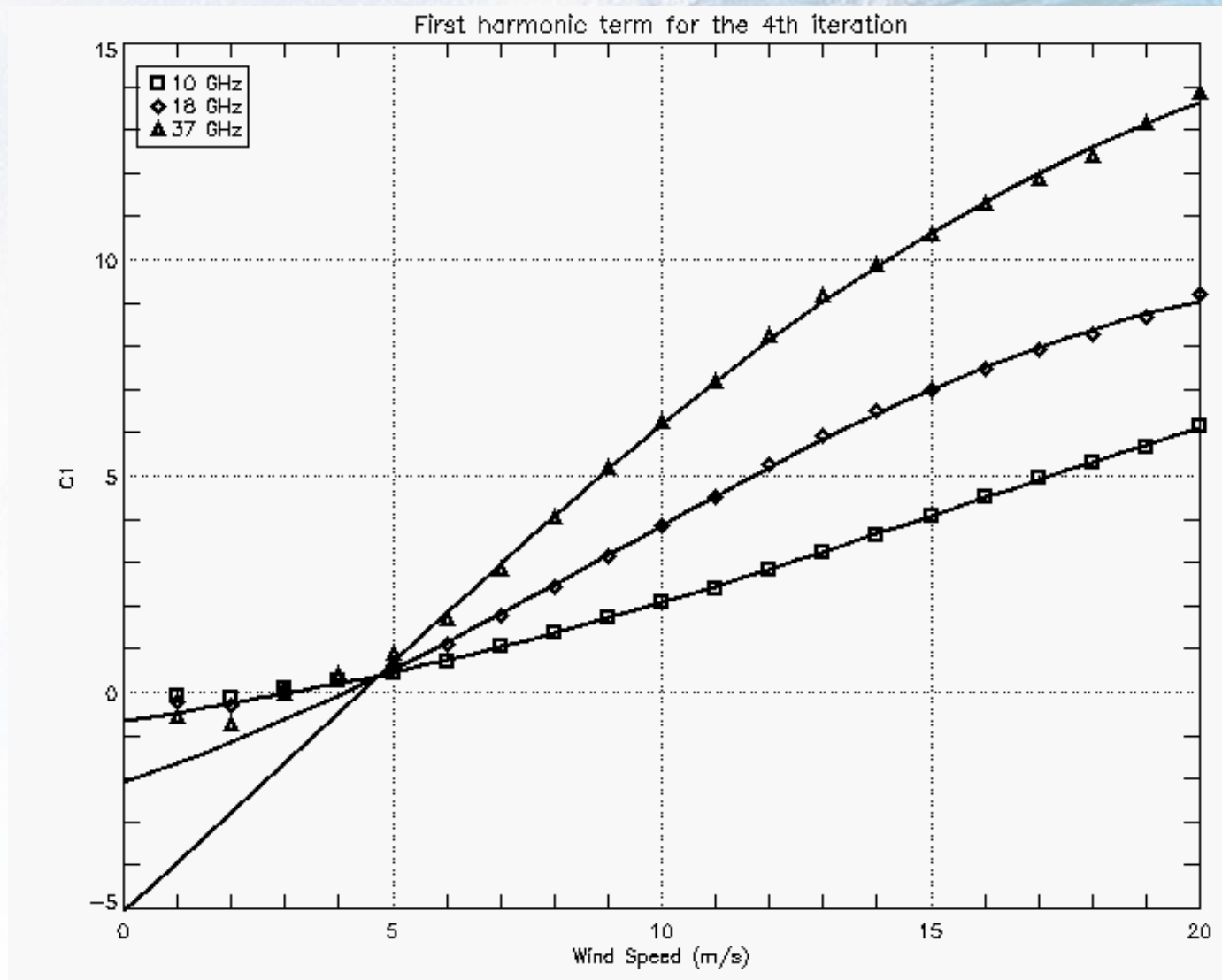
Model Function for 18 GHz



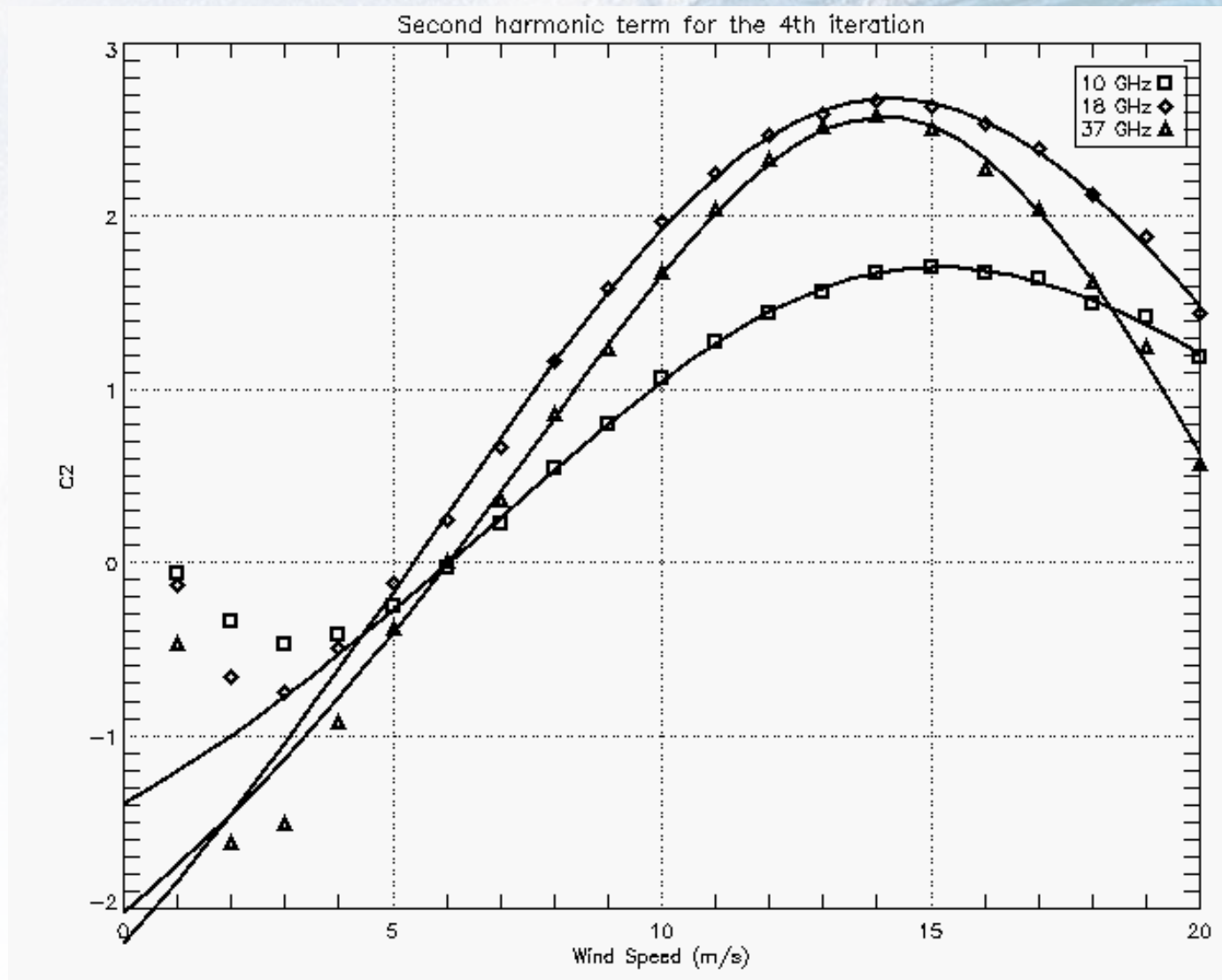
Model Function for 37 GHz



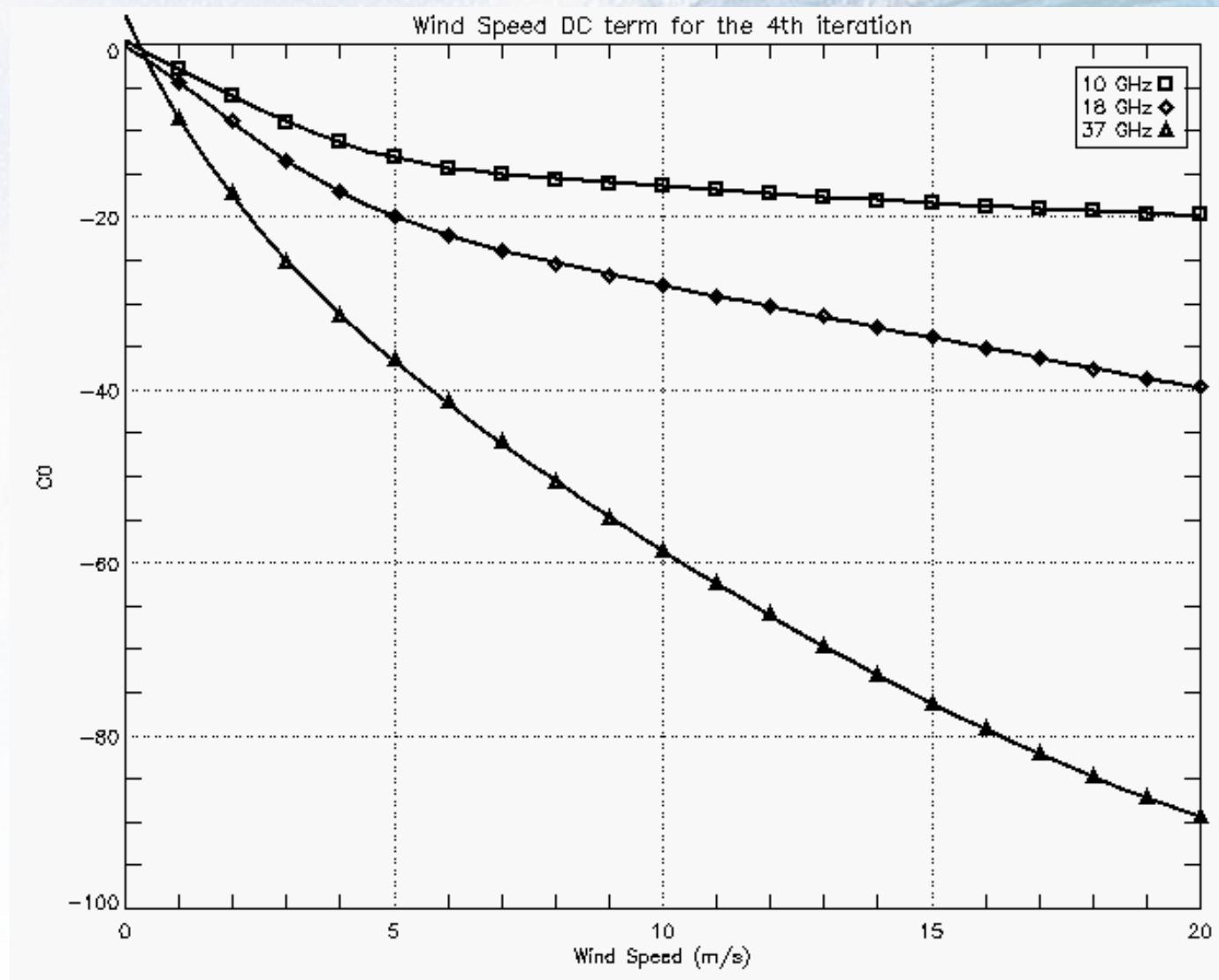
Coefficient C_1



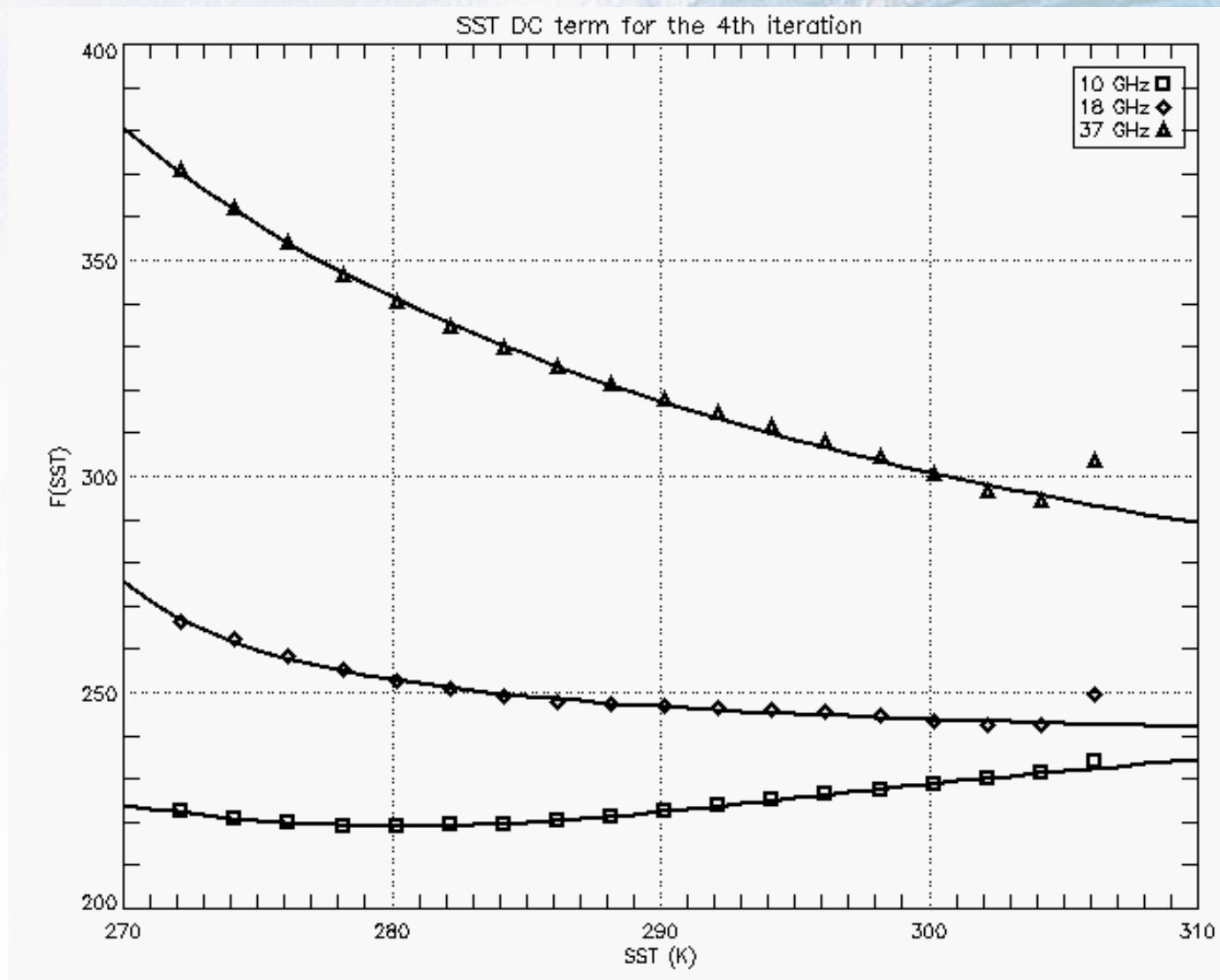
Coefficient C_2



Wind speed dependence dc



SST dependence dc



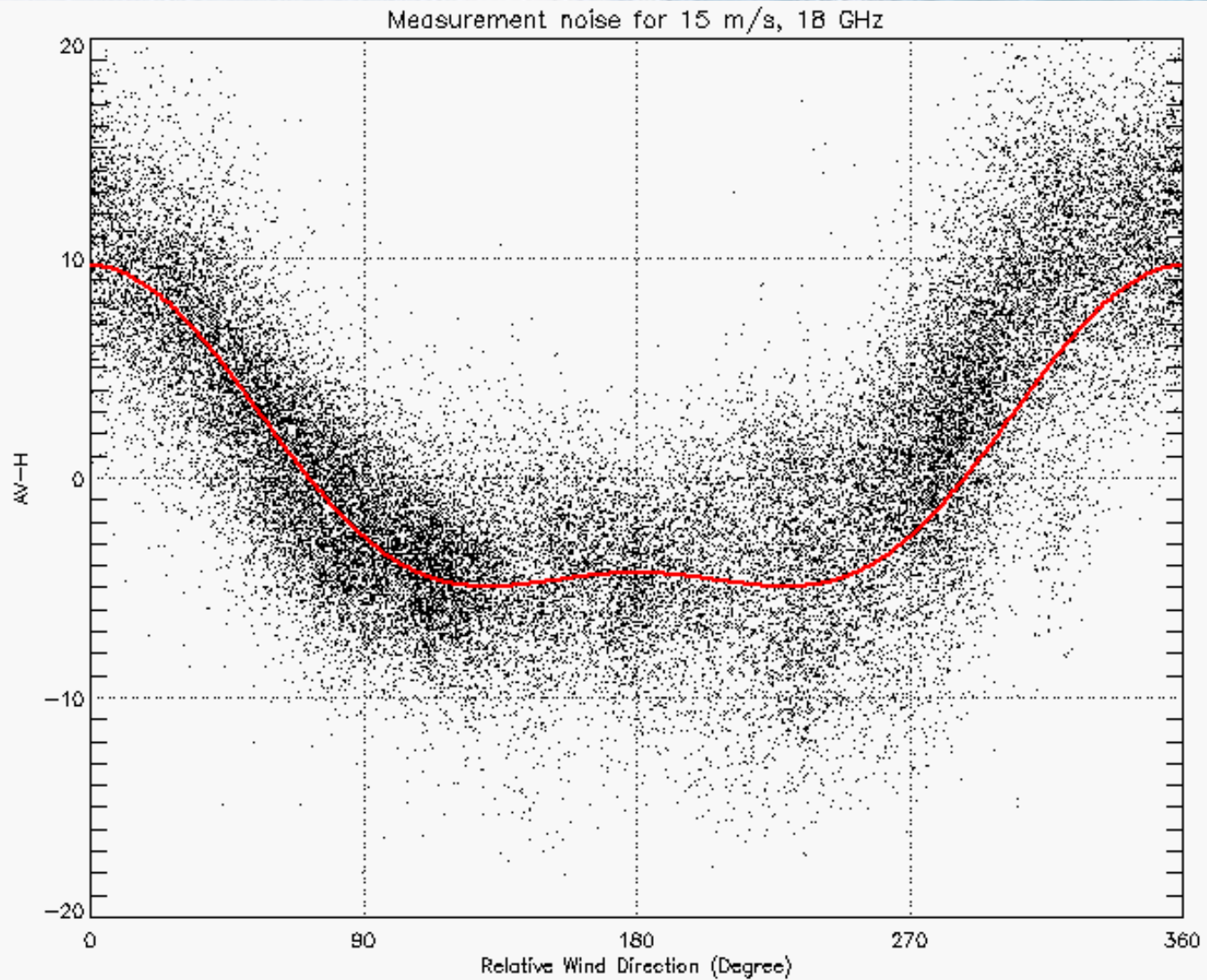
Model standard deviation

- Directional model standard deviation was found as a function of relative direction and wind speed
- Standard deviation was model the same way as the model function in the form

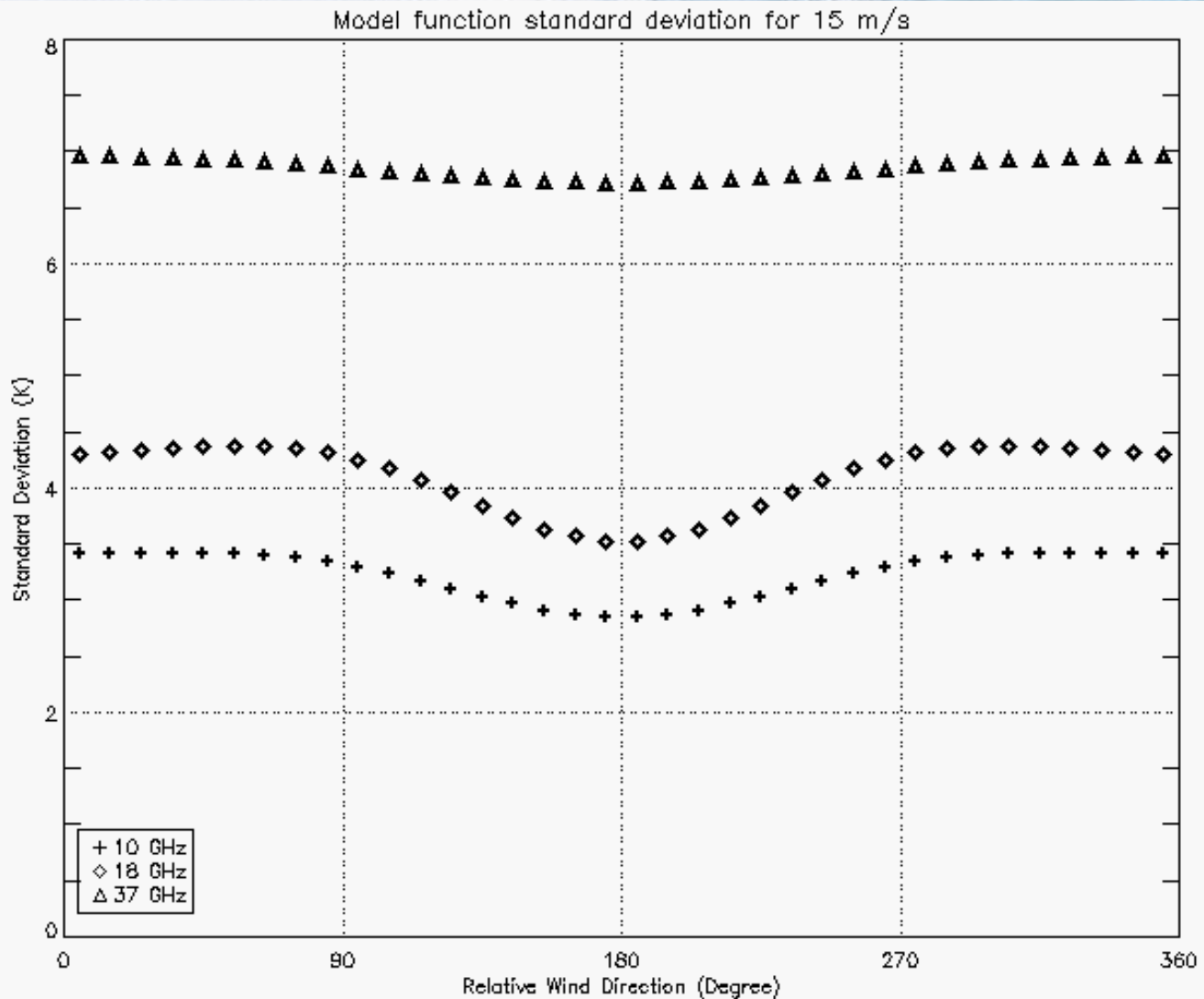
$$STD = C_1(WSPD) \cdot \cos(\chi) + C_2(WSPD) \cdot \cos(2\chi)$$

- Same regression process was repeated

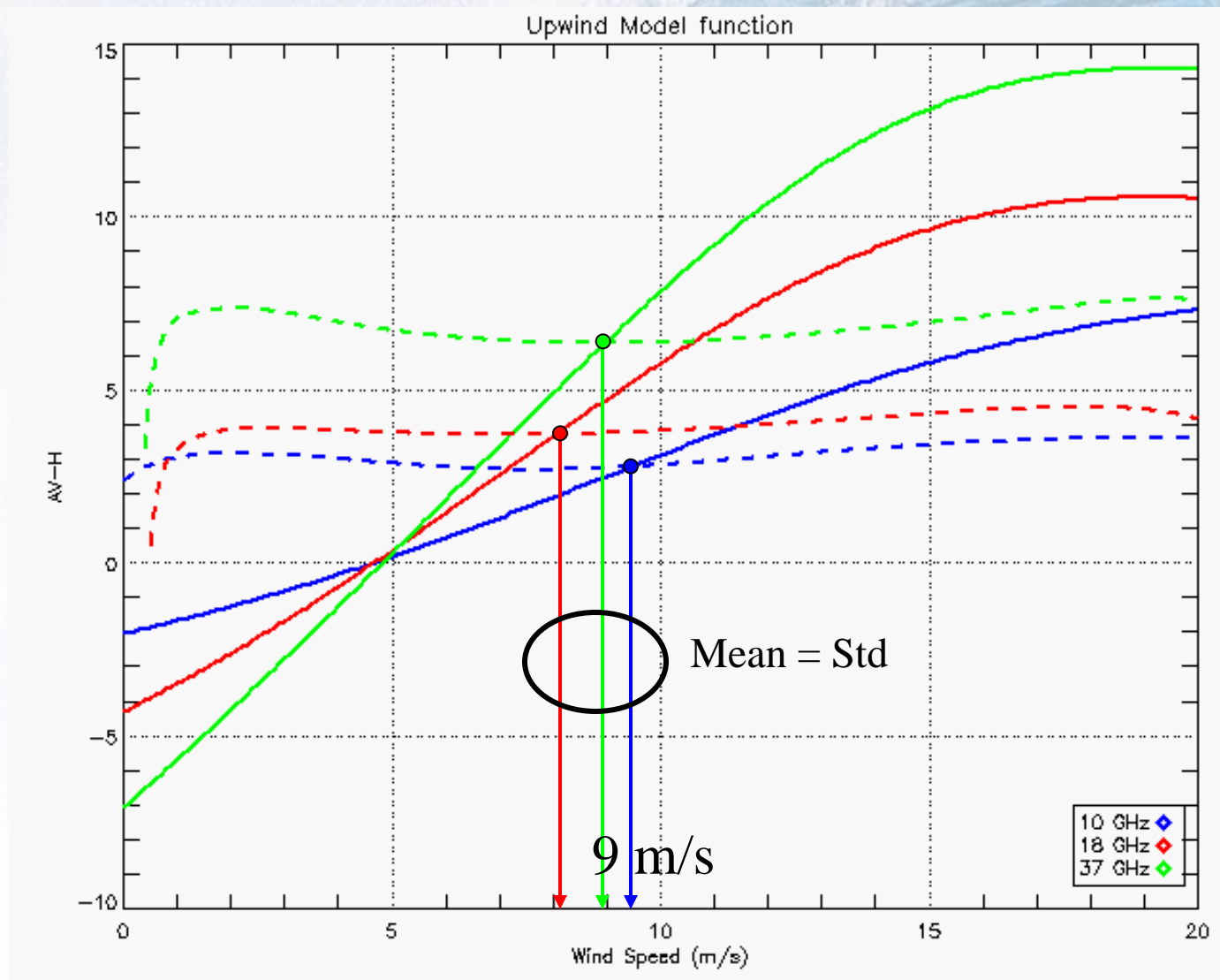
Measurement Noise



Standard deviation



Standard deviation for Upwind



Wind Vector Retrieval

- Wind vectors are ideally retrievable using the model function for AV-H measurement and given SST
- Retrieval algorithm based on maximum likelihood estimation (MLE)

$$\zeta = \sum_{freq=10,18,37GHz} \frac{\left(AVH_{Meas} - AVH_{Model}(wspd, rel.dir, SST)_{freq} \right)^2}{Variance_{AVH}(wspd, rel.dir)_{freq}}$$

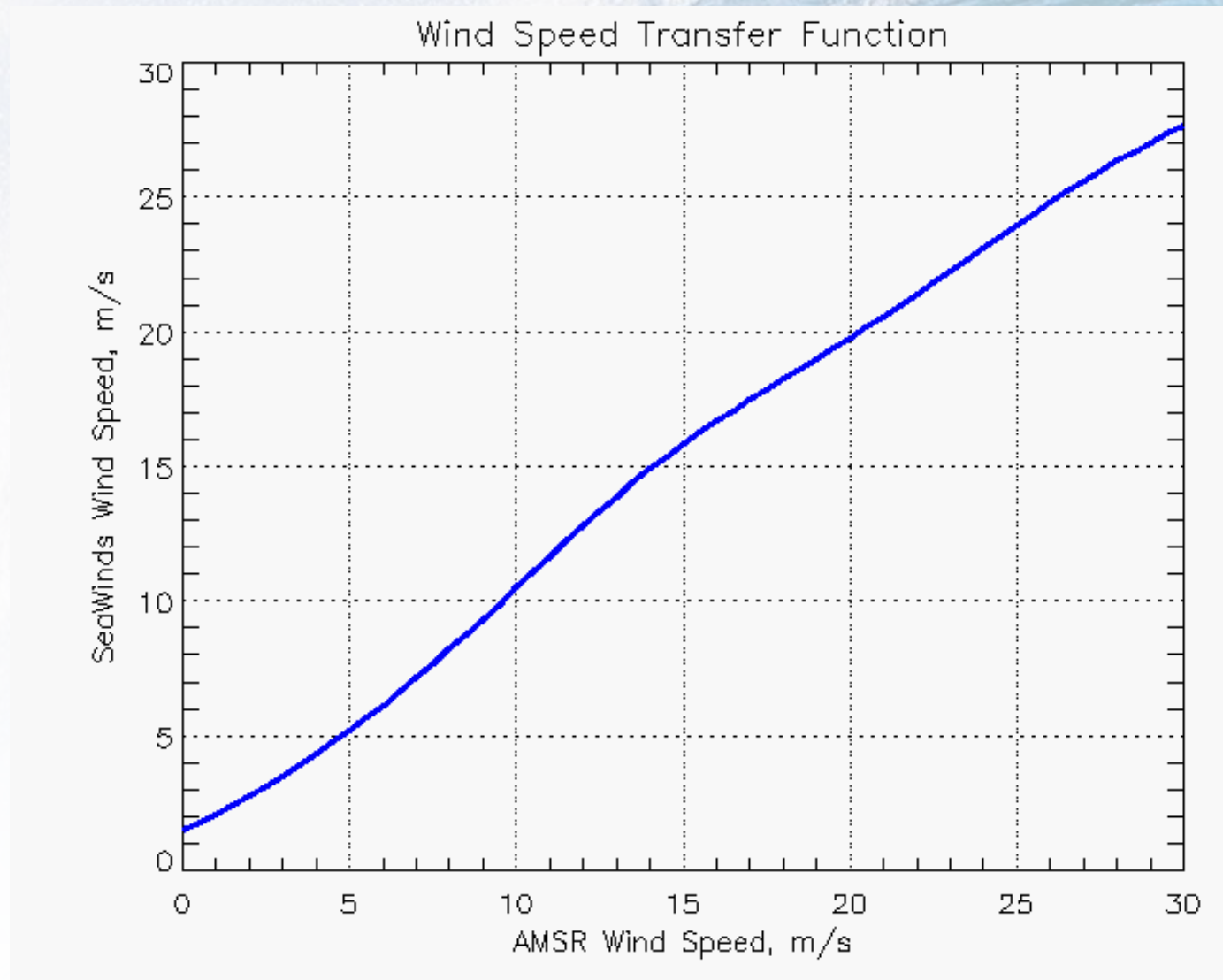
Wind Vector Retrieval -2

- In practice measurements standard deviations are relatively high for $wspd < 9 \text{ m/s}$
- Wind retrieval from AV-H alone will not achieve required accuracy
- AV-H brightness may be combined with the other measurements to be able to retrieve wind vector

Combined Active/Passive retrieval

- Use favorable geometry measurements of AMSR's T_B and SeaWinds' σ^0 on ADEOS-II
- Only fore-look σ^0 measurements were used
 - Assess usability of AV-H model function
 - Simplifies instrument design
 - Adds two feed and electronics to multi-channel conical scanning radiometer
- Given SST available from GDAS, and known wind speed retrieved from SeaWinds scatterometer

Wind speed transfer function



Active/Passive Algorithm

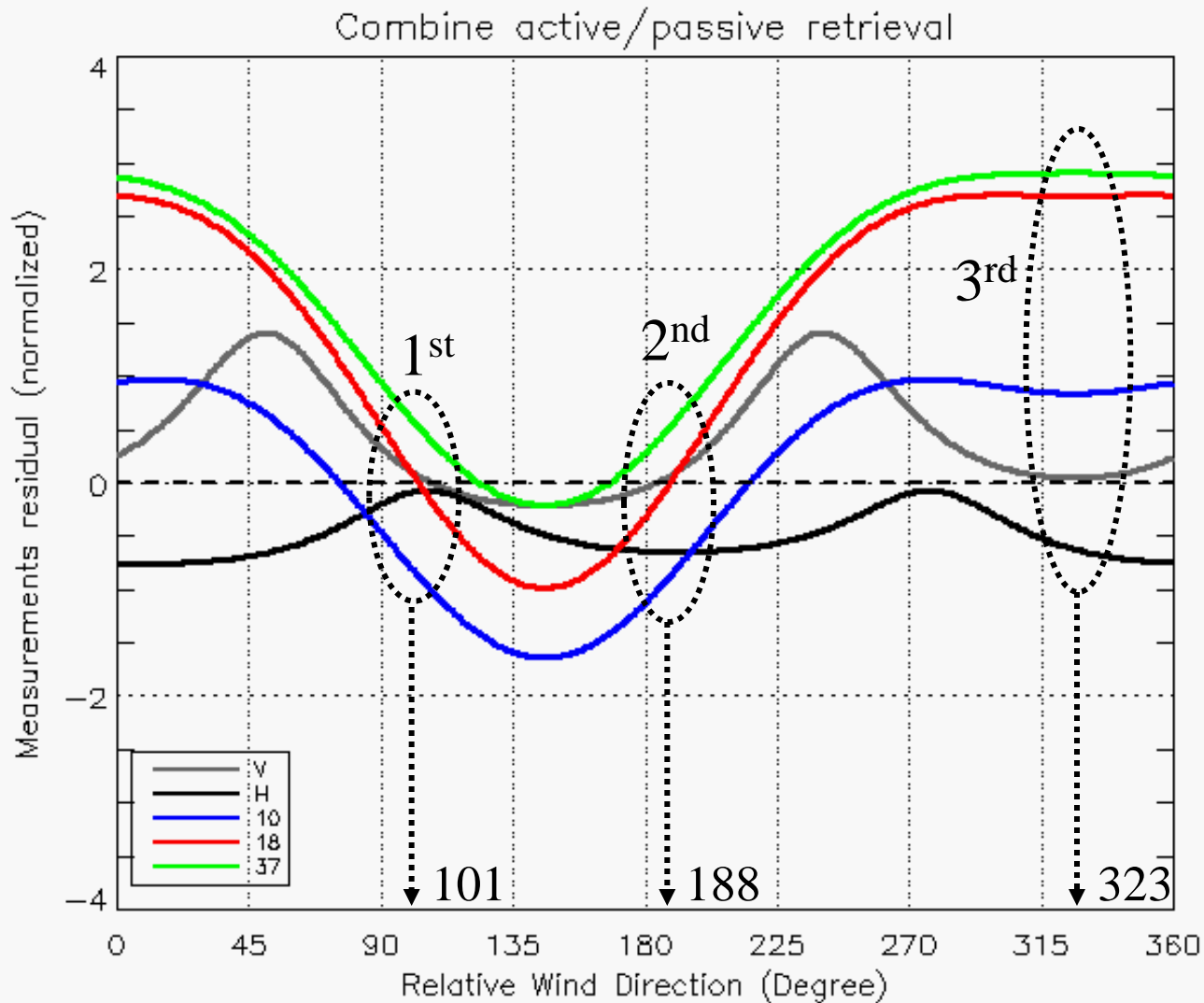
$$\zeta = \sum_{freq=10,18,37GHz} \frac{\left(AVH_{Meas} - AVH_{Model}(wspd, \chi, SST)_{freq} \right)^2}{Variance_{AVH}(wspd, \chi)_{freq}} + \sum_{pol=V,H} \frac{\left(\sigma_0 - GMF(wspd, \chi)_{pol} \right)^2}{Variance_{\sigma_0}(wspd, \chi)_{pol}}$$

$\chi = azimuth - direction$

Wind direction ambiguities

- Wind direction solution is not unique - caused by biharmonic nature of the model functions
- Wind direction solutions were kept up to four and ordered according to the inverse values of MLE
 - i.e. 1st ranked solution corresponds to minimum MLE value, 2nd ranked is the second minimum, ...
- Of these ambiguities, only one of the solutions is the “correct” wind direction

Measurements residual



Wind Retrieval Comparison

Active/Passive Retrievals

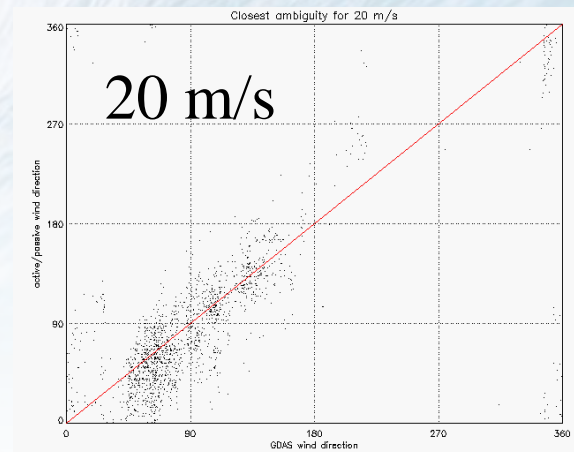
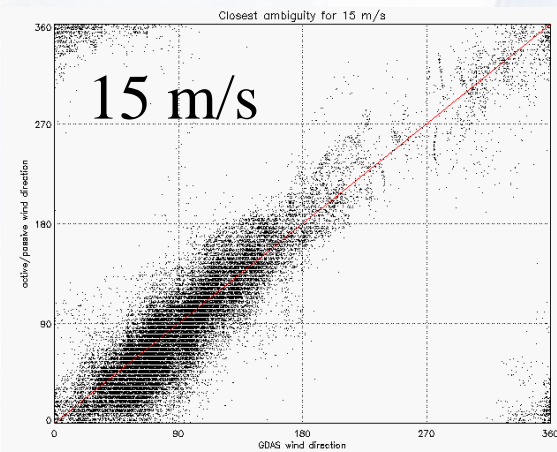
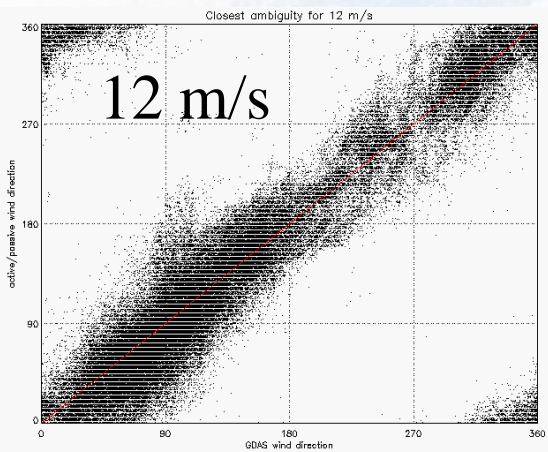
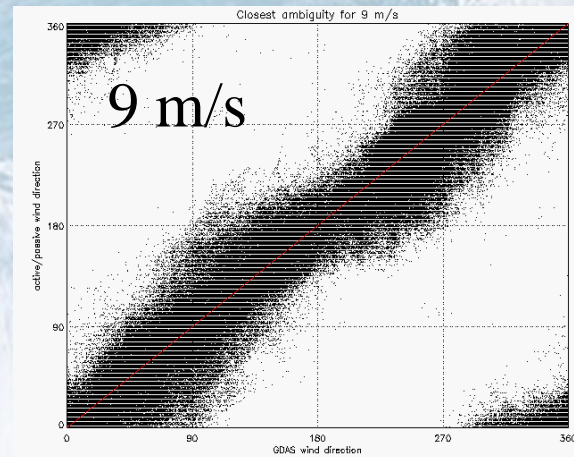
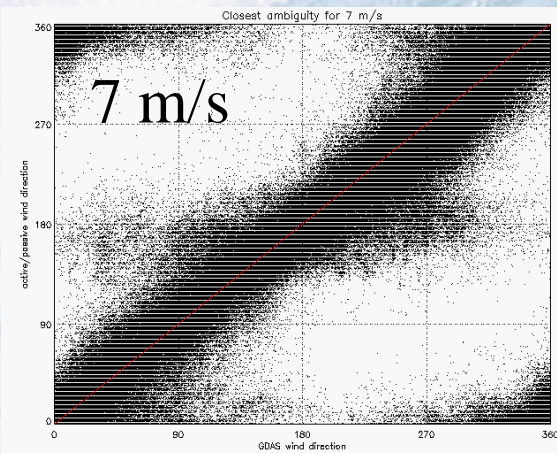
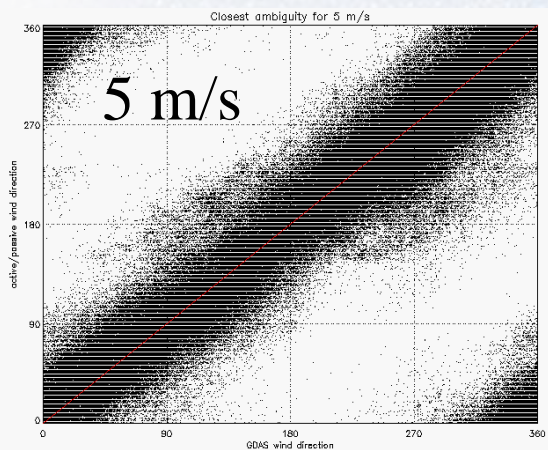
- For best case scenario, ambiguities were compared to the known surface truth and the closest direction solution was selected
- GDAS was used as the surface truth (independent source)

Active fore-look

- Wind direction comparisons were also made for the “closest” solution retrieved without using passive AV-H measurements

Closest Ambiguity Comparison

↑ Active/Passive direction



GDAS direction



Closest solutions comparison

Wind Speed (meter/sec)	Number of Points	Closest Ambiguities: Standard Deviation Error	
		Passive + fore-look Scat	Only fore-look Scat
5	337493	20.8°	14.1°
7	441818	23.6°	10.8°
9	309717	17.4°	9.0°
12	99563	17.5°	9.0°
15	33520	17.1°	9.5°
20	1680	19.1°	13.7°

Current scatterometer is capable of wind speed measurement of 3-20 m/s

- wind speed accuracy: 2 m/s
- wind direction accuracy: 20°

Instrument Skill

- The instrument skill is a metric to determine the performance of the wind ambiguity removal based upon ambiguity ranking
- The higher the probability that 1st ranked solutions are the closest solution, the greater the skill of the instrument
- Usually in four-look scatterometry, the 1st and 2nd ranked solutions are the most probable closest wind vector

Skill Comparison

Wind Speed (meter/sec)	Closest Ambiguity Ranking							
	Passive + fore-look Scat				Only fore-look Scat			
	1 st	2 nd	3 rd	4 th	1 st	2 nd	3 rd	4 th
5	30 %	35 %	23 %	13 %	26 %	30 %	29 %	15 %
7	30 %	34 %	23 %	13 %	22 %	27 %	32 %	18 %
9	30 %	37 %	27 %	6 %	25 %	27 %	33 %	15 %
12	61 %	28 %	10 %	1 %	50 %	30 %	13 %	7 %
15	82 %	15 %	2 %	1 %	63 %	29 %	5 %	3 %
20	91 %	9 %	0 %	0 %	69 %	25 %	2 %	4 %

Skill Comparison

Wind Speed (meter/sec)	Closest Ambiguity Ranking							
	Passive + fore-look Scat				Only fore-look Scat			
	1 st	2 nd	3 rd	4 th	1 st	2 nd	3 rd	4 th
5	30 %	35 %	23 %	13 %	26 %	30 %	29 %	15 %
7	30 %	34 %	23 %	13 %	22 %	27 %	32 %	18 %
9	30 %	37 %	27 %	6 %	25 %	27 %	33 %	15 %
12	61 %	28 %	10 %	1 %	50 %	30 %	13 %	7 %
15	82 %	15 %	2 %	1 %	63 %	29 %	5 %	3 %
20	91 %	9 %	0 %	0 %	69 %	25 %	2 %	4 %

Active/Passive Skill Improvement

Wind Speed (m/s)	Skill improvement (1 st and 2 nd rank combined)	Standard deviation	
		Only fore-look Scat	Passive + fore-look Scat
5	9 %	14.1 °	20.8 °
7	15 %	10.8 °	23.6 °
9	15 %	9.0 °	17.4 °
12	9 %	9.0 °	17.5 °
15	5 %	9.5 °	17.1 °
20	6 %	13.7 °	19.1 °

Conclusion

- Linear combination of vertical and horizontal brightness temp. ($AV-H$) is a function of only surface parameters
 - A is a $f(\text{Freq, pol, SST and wind speed})$
 - Effects of atmosphere cancel
 - Large DC bias is $f(\text{Freq, pol, SST and wind speed})$
- Empirical relationship between $AV-H$ and surface parameter is defined for wind vector and SST.

Conclusion -2

- Measurement noise (ΔT_b) dominates over wind directional signal for wind speed < 9 m/s
 - May prevent wind retrieval using passive measurement alone
- Combined active and passive has been investigated with fore-look geometry
 - Closest ambiguity shows that retrieval achieves wind direction accuracy of $< 20^\circ$
 - However, wind direction accuracy degrades compared to closest fore-look active measurement alone
 - But, instrument skill is higher (than using fore-look active measurement alone)

List of Conf. Publications

- Jones, W.L., Soisuvarn, S., Kasparis, T., and Ahmad, S., “Combined Active And Passive Microwave Sensing Of Ocean Surface Wind Vector From TRMM”, AGU Spring Meeting, May 28-31, 2002, Washington, DC
- Jones, W. L., Soisuvarn, S., Kasparis, T., Ahmad, S. and R. Meneghini, “Ocean Surface Wind Speed Measurements Using The TRMM Precipitation Radar”, International Tropical Rainfall Measuring Mission (TRMM) Science Conference, Jul 22-26, 2002, Honolulu, HA.
- Soisuvarn, S., Jones, W. L. and T. Kasparis, “Combined Active And Passive Microwave Sensing Of Ocean Surface Wind Vector From TRMM”, Oceans '02 MTS/IEEE, Oct 29-31, 2002, Biloxi, MS.
- Soisuvarn, S., Jones, W. L. and T. Kasparis, “Combined Active And Passive Microwave Sensing Of Ocean Surface Wind Vector From TRMM”, IGARSS '03, Jul 21-25, 2003, Toulouse, France.
- Soisuvarn, S., Jones, W. L. and T. Kasparis, “Validation Of Ocean Surface Wind Vector Sensing Using Combined Active And Passive Microwave Measurement”, IGARSS '04, Sep 20-24, 2004, Anchorage, AK.

List of Conf. Publications -2

- Soisuvarn, S., Jones, W. L., T. Kasparis, “Ocean Surface Wind Vector Retrievals Using Active And Passive Microwave Sensing On ADEOS-II”, IGARSS '05, Jul 25-29, 2005, Seoul, Korea
- Jones, W. L., and S. Soisuvarn, “A Novel Active and Passive Microwave Remote Sensing Technique for Measuring Ocean Surface Wind Vector”, Oceans '05 MTS/IEEE, Sep 18-23, 2005, Washington, DC
- Soisuvarn S., Jones, W. L, and Z. Jelenak, “A Novel Oceanic Wind Vector Measurement from ADEOS-II using Combined Active and Passive Microwave Techniques”, AGU Joint Assembly, Baltimore, Maryland, 23-26 May 2006
- Soisuvarn S., Jones, W. L, and Z. Jelenak, “Development of Oceanic Wind Vector Model Function for AMSR Radiometer on ADEOS-II Satellite”, Proc. IEEE IGARSS-06, Aug. 28 - Sept. 1, 2006, Denver, CO.

Refereed Publications

- W. Linwood Jones, Jun D. Park, **Seubson Soisuvarn**, Liang Hong, Peter Gaiser and Karen St. Germain, “Deep-Space Calibration of WindSat Radiometer”, *IEEE Trans. GeoSci. Rem. Sens.*, Vol. 44, NO. 3, Mar 2006
- **S. Soisuvarn**, Z. Jelenak and W. L. Jones, “An ocean surface wind vector model function for a spaceborne microwave radiometer,” *IEEE Trans. Geosci. Remote Sensing* (submitted Sept 2006; under peer review)